High-Resolution Climate Change Projections for the City of Edmonton

Final Report
May 2021

Principal Investigator: David Sauchyn, PhD, PGeo

Research Associates: Muhammad Rehan Anis, PhD; Yuliya Andreichuk, MASc; Soumik Basu, PhD

Graduate Research Assistant: Samantha Kerr, PhD

Project Sponsors:

Acknowledgments:

Funding for the research described in this report was an IPCC Cities Legacy Research Grant administered by Alberta EcoTrust and an NSERC grant from the Collaborative Research and Development program. We acknowledge the role of Simon Irving from AB EcoTrust. The research was done in support of the City of Edmonton's Climate Change Adaptation and Resilience Strategy. Danielle Koleyak, Environmental Project Manager with City Environmental Strategies, was our contact. Ms. Koleyak facilitated meetings and referred the researchers to relevant information and personnel. We appreciated her assistance. This project also benefited from our relationship with EPCOR Water Canada and their support of closely related research on the impacts of climate change on the North Saskatchewan River.

Citation: Sauchyn, David; Soumik Basu, Muhammad Rehan Anis, Yuliya Andreichuk, and Samantha Kerr (2021) High-Resolution Climate Change Projections for the City of Edmonton, Final Report to Alberta EcoTrust and the City of Edmonton.

TABLE OF CONTENTS

FIGURES

TABLES

1 Introduction

The goal of the research project "High-Resolution Climate Change Projections for the City of Edmonton" was to provide scientific support for the City's Climate Change Adaptation and Resilience Strategy (City of Edmonton, 2018) with projections of the future climate of the Edmonton Municipal Region (EMR) at high spatial and temporal resolution; thereby assisting planners, engineers, managers and policy makers with decision-making for an uncertain future. Climate projections are the basis for evaluating climate risks to municipal assets and public services in terms of the probability of exceeding critical thresholds in weather and water variables. We are prepared to supply City of Edmonton (CoE) staff with guidelines for translating the climate projections and uncertainties for engineering and planning applications.

An innovative aspect of the project is climate change projections at relevant scales of space and time, and within the context of the requirements of the CoE. Various scientific papers and reports (e.g., AOS Foundation, 2018; CRC Climate Resilience Consulting, n.d.; Golder Associates, 2008; Jiang et al., 2017; Kienzle et al, 2012; MacDonald et al., 2012) describe variability and change in the climate and hydrology of central Alberta. In every case, the climate change projections were based on output from Global Climate Models (GCMs) with a large degree of uncertainty, especially for the projection of regional precipitation and climate extremes.

Despite a critical need for climate projections at a city scale, high-resolution climate projections, especially of the frequency and magnitude of extreme events, are not available for the Edmonton region. Similarly, hydrological models of the North Saskatchewan River Basin (NSRB) have been run using climate data from statistically downscaled GCMs. Statistically downscaling by linking local weather to variables representing large-scale atmospheric processes is a spatial interpolation of global model data to a finer scale; however, the numerical simulation of climate processes remains at the coarse scale of the GCM. Whereas climate projections derived from GCMs are adequate for raising awareness of climate change and informing a policy response, data of higher resolution in time and space are required to support asset risk management and civil engineering.
Thus the research reported here fills a knowledge gap in terms of the scale and type of information required to implement adaptation plans for Canadian cities, with Edmonton as the case study. Our partners at the City of Edmonton (CoE) are implementing an ambitious climate change adaptation and resilience strategy that requires the type of scientific support documented in this report. Edmonton's climate

adaptation strategy refers explicitly to the use of formal climate science and to evidence based policy and decision-making.

Given the natural (e.g., the large river valley) and socio-economic diversity of a major city like Edmonton, the impacts of climate change and extreme events will differ among neighbourhoods. Climate modeling and analysis at this scale is computing intensive. There is a trade-off between the availability of large amount of climate model data at coarse resolution and relatively little data at high resolution. This project produced a novel set of climate model data of sub-daily and 3.3 km resolution, requiring months of computing on one of Canada's most powerful computers[1].

The project's major deliverable is climate change data for City of Edmonton of unprecedented high resolution. This data set was derived by dynamical downscaling of output from a single run of the Community Earth System Model (CESM). To offset the uncertainty associated with deriving climate data from a single experiment; we interpret the results of our high-resolution climate modeling within the context of other climate projections for the Edmonton region. These other climate are from RCMs of lower resolution (25 km) but still much higher than the GCMs previously used to generate climate projections for central Alberta.

This project supports science-based planning and policy to improve the resilience of economies and communities given projected changes in climate. Urban planning and policy are now viewed through a climate change lens, requiring climate data for relevant variables and scales. In developing its climate adaptation strategy and action plan, the CoE identified key climate variables and indices, making a distinction between the sudden versus slow onset of climate driven changes. By defining these critical variables and indices, they created a framework for evaluating thresholds beyond which climate conditions become hazardous. Determining the probability of exceeding these thresholds, for the sudden onset variables (e.g., extreme stormwater runoff) in particular, require data of higher spatial and temporal resolution than currently available. Our project provides this information. We also will advise city planners, engineers, managers and policy makers on the best practices for using climate model projections and dealing with the inherent uncertainty. We can advise them about the validity of continuing to use primarily historical weather and water data, which are the conventional basis for science-based decision making.

In addition to this technical report, a brief synthesis report for use by a larger group of stakeholders will summarize the findings, and communicate concepts of climate change and variability, risk, uncertainty, resilience and adaptation using locally relevant examples and illustrations. As a university-based research center, and a founding partner of ClimateWest[2], the Prairie Provinces hub in the Canadian Centre for Climate Services, PARC is strategically situated to provide training in climate

[1] PARC researchers have access to Canada's most powerful academic supercomputers including Cedar at Simon Fraser University – see https://www.sfu.ca/research/supercomputer-cedar

[2] https://climatewest.ca/

change science and its application to adaptation policy and planning. The widespread recognition of unavoidable climate change has raised the profile of adaptation as an essential policy response to climate change. In general, urban municipalities are the level of government where this is most evident. With the mainstreaming of climate adaptation planning, and recognition of climate risk as an important decision making criterion, there is a growing demand among practitioners for a common understanding of the science of climate change, risk and impact assessment, adaptation principles and best practices. Relatively few professional social scientists, engineers, planners and policy makers have post-secondary education and training related to climate change. Therefore a key component of the proposed project is to provide the partner organization with advice for implementing the climate change science and knowledge generated by the project.

1.1 Timelines / Milestones

The research described in this report followed the timeline outlined in Table 1. The project was on schedule until March 2020 when COVID pandemic restrictions were first imposed. Since then the research team has had limited access to our labs and offices at the University of Regina. Remote access to computing facilities enabled us to complete the technical work on schedule. However, aspects of research requiring consultation with our project partners are delayed. While we have maintained communication with our contacts at the City of Edmonton via e-mail and virtual meetings, a knowledge translation workshop and plain language synthesis is a waiting on a lifting of restrictions on travel and meetings.

Table 1: The Original Project Timeline.

Activity	Description	Dates
Consulting with CoE	Reviewing project objectives, deliverables and expectations, and framing Alliance proposal from the perspective of the partner organization	12/01/2019 – 12/15/2019
Compile data	Access and compile historical weather and water data, and output from the most recent runs of Regional Climate Models	12/15/2019 –02/30/2020
Analysis of instrumental data	Analyze historical weather data for trends and variability, and frequency of extremes that exceed locally relevant thresholds	02/01/2020 – 04/30/2020
Dynamical downscaling	Implementing the WRF model with 6 hourly bias-corrected output from the Community ESM	03/01/2020 – 8/31/2020
Validation / bias correction of climate model projections	Compare output from historical runs of CORDEX RCMs to weather observations for the same historical period; apply a bias correction algorithm	3/01/2020 – 05/31/2020
Analysis of paleohydrology	Updating our 900-year tree-ring reconstruction of annual hydroclimate at Edmonton; scaling to weekly estimates	03/01/2020 – 06/30/2020

Develop high-resolution climate projections	Derive from an ensemble of RCMs climate projections for key climate and water variables	05/01/2020 – 08/31/2020
Mapping and analysis of WRF output	Mapping, analyzing and plotting high-resolution (3.3 km) output from the WRF model; generate climate projections for key variables	9/01/2020 – 12/31/2020
Uncertainty analysis	Attribute differences among climate projections to the use of different models and emission scenarios, and to natural variability as captured in our tree-ring reconstruction of the pre-industrial climate	08/01/2020 – 12/31/2020
Analysis of extreme events	Statistical analysis of the ensemble of climate projections to determine the probabilities of exceeding critical thresholds	09/01/2020 – 12/31/2020
Hydrological simulation	Driving the MESH hydrological model with RCM climate change projections	09/01/2020 – 11/30/2020
Analysis of MESH model output	The analysis and interpretation of projections of river flooding and stormwater runoff	12/01/2020 – 02/28/2021
KT workshop	A project-ending workshop to deliver and translate the final results, and apply them to an assessment of potential climate risks	02/15/2021
Compiling and reporting of final results	A comprehensive final report and delivery of data, with research results and recommendations for their use	01/01/2021 - 04/30/2021
Compile plain language summary	A plain language summary to communicate the results and implications for policy makers and the public	03/01/2021 – 04/30/2021
Publish and present	Publish the research results in referred journals and present them at national conferences	01/01/2020 – 05/31/2021

2 Historical Climate Trends at Edmonton

Long weather records are vital for understanding variability and change in regional hydroclimates. Thus climate change research in Canada is enabled by Adjusted and Homogenized Canadian Climate Data (http://ec.gc.ca/dccha-ahccd/) (AHCCD). These data incorporate a number of adjustments applied to the original weather station records to address shifts due to changes in instruments and in observing procedures (Vincent et al. 2012; AHCCD, 2017). Figure 1 is a time series of mean annual temperature recorded at Edmonton since 1884. Annual temperatures have averaged between -1° C and 5° C. In addition to large differences in temperature between years, there are also consecutive years of warmer (e.g., mid 80s to early 90s) and cooler (e.g., mid 60s to mid 70s) weather. This natural variability from year-to-year and decade-to-decade tends to obscure a statistically significant upward trend. Nevertheless, the region is getting warmer; mean annual temperature has risen by about 2° C.

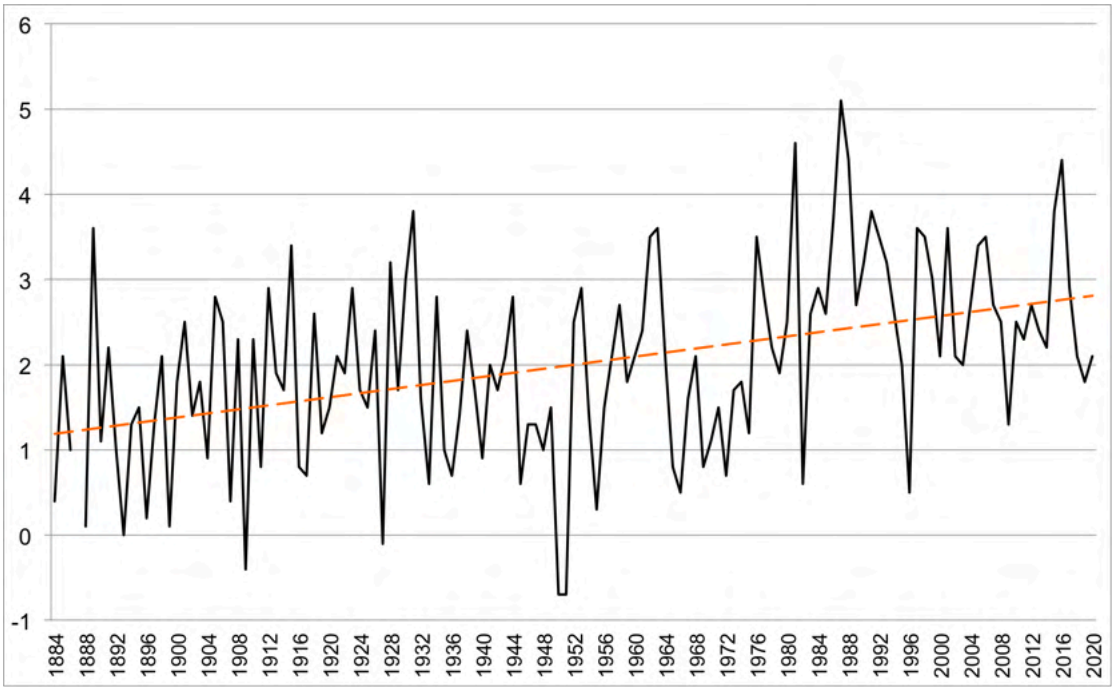

Figure 1: Mean annual temperature (° C) at Edmonton since 1884 and the linear upward trend.

While Figure 1 reveals a statistically significant increase in average annual temperature, these data averaged for the whole year hide an important fact; most of the warming is occurring in winter to the lowest temperatures. Thus, western Canada is not getting hotter; it is getting much less cold as illustrated in Figures 2 and 3. The highest temperatures have increased only slightly; the linear trend in Figure 3 represents a rise in mean daily maximum summer (JJA) temperature of less than 1º C from 1882 to 2020. The hottest summers were during the driest years such as 1961.

The lowest temperatures, on the other hand, have increased dramatically. Figure 3 is a plot of mean daily minimum winter (DJF) temperature at Edmonton from 1884 to 2020. There is large natural variability around a steep upward trend of 6.5° C. The warmest winter was in 1931 during a very strong El Niño. Over the past three decades, the two coldest winters had a mean daily minimum temperature of approximately -20° C. These would have been average winters for most of the 20th century.

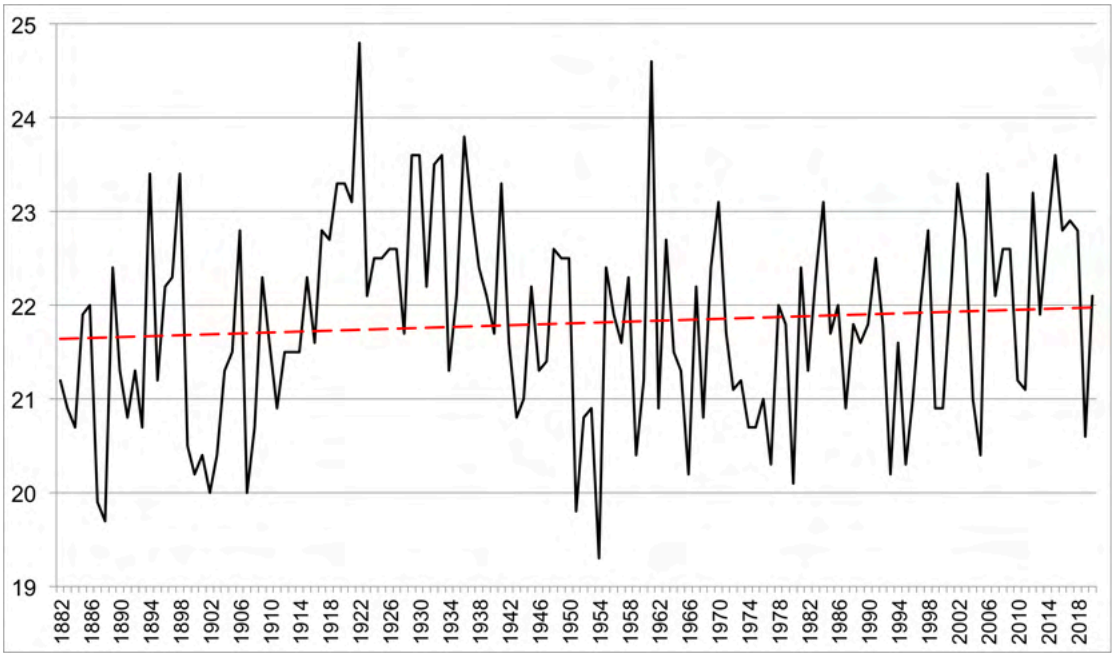

Figure 2: Mean daily maximum summer (JJA) temperature (º C) at Edmonton, 1882-2020.

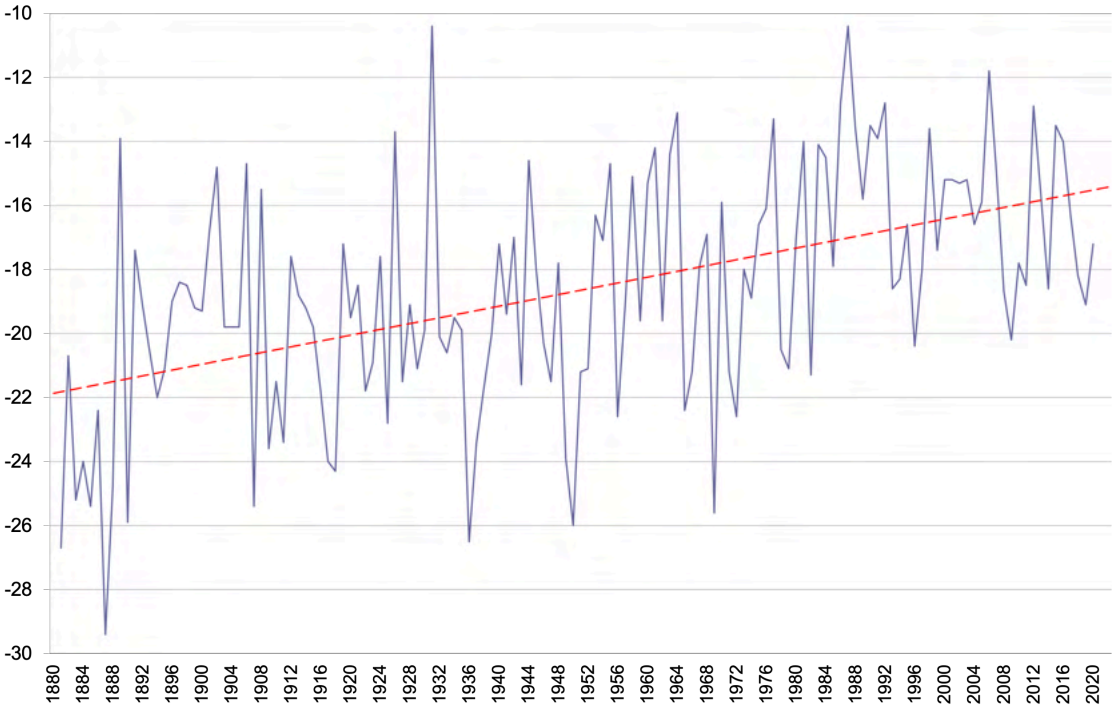

Figure 3: Mean daily minimum winter (DJF) temperature (ºC) at Edmonton, 1884-2020.

Total annual precipitation at Edmonton ranges from 250 to 800 mm. The annual cycle of monthly precipitation is graphed in Figure 4. The wettest months are June and July.

The range of precipitation is widest in the summer months (JJA) indicating a higher year-to-year variability than in the other seasons. Thus, total annual precipitation depends mostly on how much rain falls in May to August. Even though most of the precipitation occurs in spring and early summer, winter precipitation (mostly snow) is more effective in generating soil moisture and runoff, since much of the summer rainfall is lost by evapotranspiration.

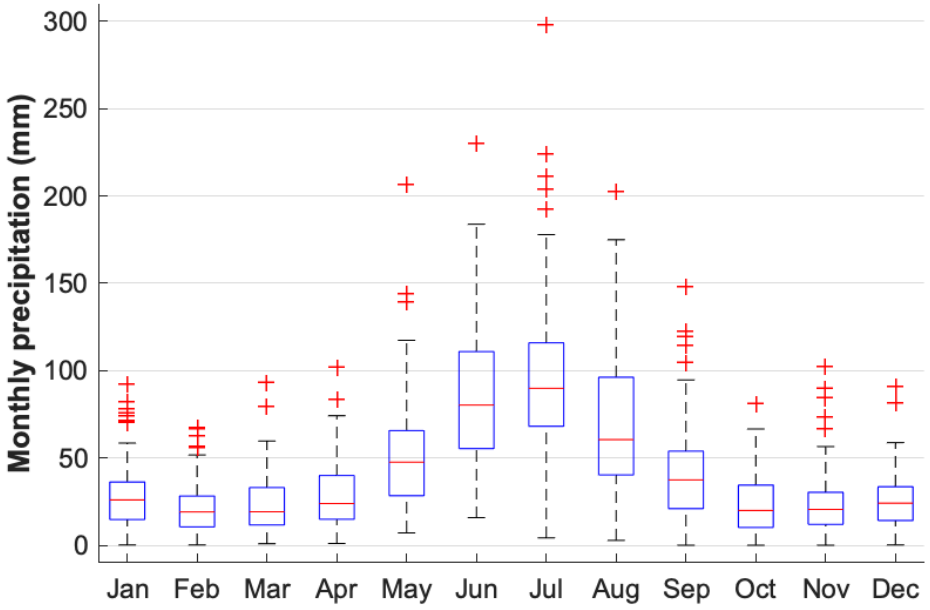

Figure 4: The annual cycle of monthly precipitation at Edmonton. The boxes represent the interquartile range (25-50%) with the red line depicting the median value. The dashed whiskers show the full range of the data with the exception of the outliers marked with red crosses.

Figure 5 is a times series plots of total seasonal precipitation at Edmonton since 1883. The linear trends indicate a long-term rise in winter precipitation and no trend in summer. Precipitation appears to be rising in spring and fall; however, the increases are insignificant relative to the large range between years. In western Canada, much of the inter-annual / decadal variability in the regional hydroclimatic is driven by its strong teleconnection with the El Niño Southern Oscillation (ENSO) / Pacific Decadal Oscillation (PDO). The extreme phases of ENSO are inversely related to precipitation during the cold season: El Niño (La Niña) is associated with below (above) average precipitation (Basu et al., 2020). There is a strong negative relationship between the PDO and streamflow in western Canada; thus water levels are higher when the PDO is in its negative phase and drier when the PDO is positive.

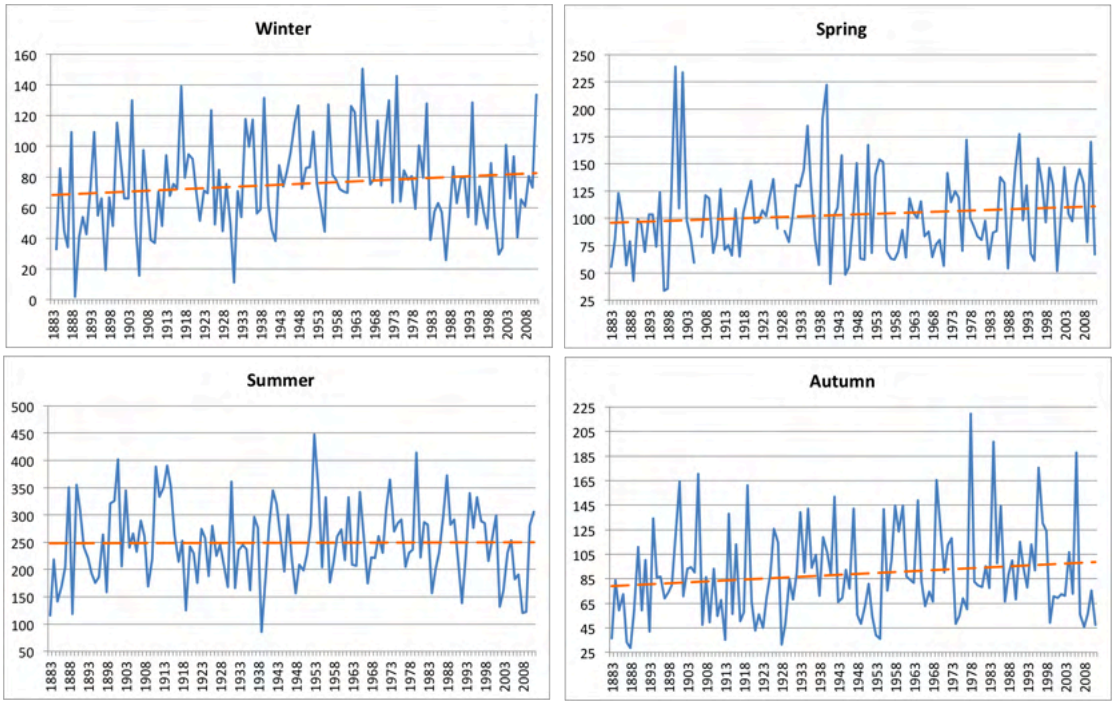

Figure 5: Total seasonal precipitation (mm) at Edmonton since 1883-2011 with linear trends.

3 Regional Climate Model Projections

3.1 The Climate Models

Climate models "are the only credible tools currently available for simulating the response of the global climate system to increasing greenhouse gas concentrations" (IPCC, 2013). They consist of a large set of differential equations that solve for the flux of mass, energy and momentum through time and space. Working from theory and observation, modellers derive the mathematical expressions that best describe the earth's climate and then solve them on a three-dimensional grid. Integrating the equations over the globe and many years enables the simulation of global climate change. There are no exact or analytic solutions to these equations, because the climate system is far too complex, and therefore numerical methods are used to arrive at approximate solutions. The numerical solutions are applied to discrete units, grid cells defined by latitude and longitude, height for the atmosphere, and depth for the oceans. According to the fundamental principal of integral calculus, the shorter the intervals of time and space (i.e., as they approach zero) the most exact the solution. In their attempt to achieve the most accurate simulations, climate modellers use relatively small grid cells but very quickly encounter the limitations of computing resources. This resolution limitation accounts for much of the model-related uncertainty in the projection of climate change. The early climate models had a grid cell resolution of hundreds of kilometers. With the massive increase in computing

power over the past several decades, the resolution of Global Climate Models (GCMs) has increased from hundreds to sub-100 kilometer resolution.

Some climate processes and states extend over many cells while others occur at a sub-grid scale and therefore cannot be modeled explicitly. Climate processes at finer spatial scales than the model grid, such as cloud formation and local convection, are approximated or parameterized according to physically based relationships with larger-scale variables. Parametrization, and model grid spacing, are issues of spatial scale. Modellers also have to choose a time scale: the interval between calculations and the length of the experiment. If climate is the statistical distribution of weather, conditions that develop at the rate of hours to days, then a climate model must run for sufficiently long periods to generate an adequate sampling of that distribution. Simulations run for 30 to hundreds of 'model years'. The calculations are typically made as frequently as every 30 minutes and as infrequently as daily. If the weather produced by a climate model were computed every 30 minutes, simulating a century of climate would involve 1,753,152 (the number of half-hours) calculations of all model parameters at each of the thousands to millions of grid points (virtual weather stations) in the model. Thus not surprisingly completing one run of global climate model can take months on a supercomputer.

Limitations on the numerical simulation of climate include current understanding and observation of the climate system and computational resources. Even the most powerful computers impose limitations, involving trade-offs between 1) model resolution - the grid spacing and time step, 2) including or excluding certain processes or components (their relevance depends on scale), and 3) the size of an ensemble, i.e., the number of runs of a single model. Compromises made between these options are informed by the intended use of the model and thus there are several classes of models of different geographic scope and complexity, including Global Climate Models (GCMs), Earth System Models (ESMs), and Regional Climate Models (RCMs).

Output from GCMs is readily available for many runs of various models. Thus, for any region on earth, a range of projections of future climate can be generated from GCM data. The interpolation of regional climate from global models introduces a large degree of uncertainty, especially for the simulation of precipitation, internal variability and climate extremes; and for any variable that must be parameterized in the GCM. GCM or ESM data can be dynamically downscaled by transferring boundary conditions to a RCM for a climate simulation at higher resolution for a limited land area.

The use of RCM data addresses the gap, in spatial and temporal scale, between the information required for climate risk assessments and the data available from GCMs. RCMs have major advantages in regions of highly variable topography and where small-scale (sub GCM grid) forcings and processes, such as convective clouds and precipitation, are important factors. Statistical downscaling can provides reliable information for single locations where a good set of weather observations is available for calibrating the statistical function linking local weather to climate patterns

simulated by the GCM. Dynamical scaling performs better; however, for constructing higher resolution spatial fields for climate variables and processes that span grid cells; regional atmospheric physics and its interaction with land and water surfaces are deterministically simulated. These spatial details are illustrated in Figures 6 and 7 using results from our modeling of the climate of the Edmonton region as described later in this report. Figure 6 is a series of maps of mean annual temperature projections for the near future (2021-2050) at four different spatial resolutions: GCM (> 110 km), and RCM domains of 30, 10 and 3.3 km resolution. The four maps in Figure 7 show projections of near future total annual precipitation at increasingly higher resolution. In both Figures, the GCM data (upper left) represent a single climate projection over an area of 1° by 1° (about 100 x 100 km). As the resolution rises to 30 and 10 km, smaller grid cells and a more detailed spatial pattern, emerge. At a resolution of 3.3 km, the number of grid cells and thus climate projections increases to more than 900 over an area equivalent to a single GCM cell.

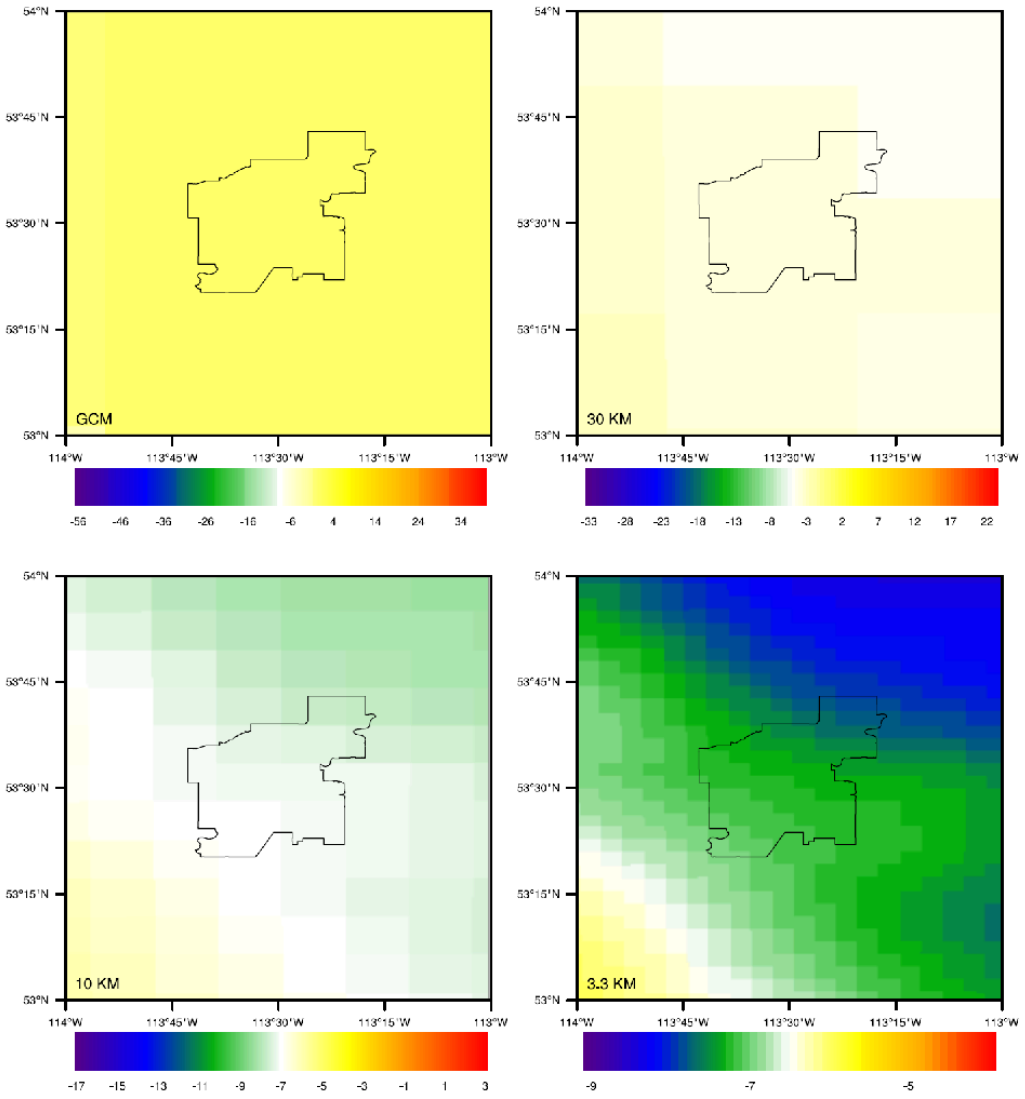

Figure 6: Model projections of the near future (2021-2050) mean annual temperature in the Edmonton region at four different spatial resolutions: GCM (> 110 km), and RCM domains at 30, 10 and 3.3 km resolution.

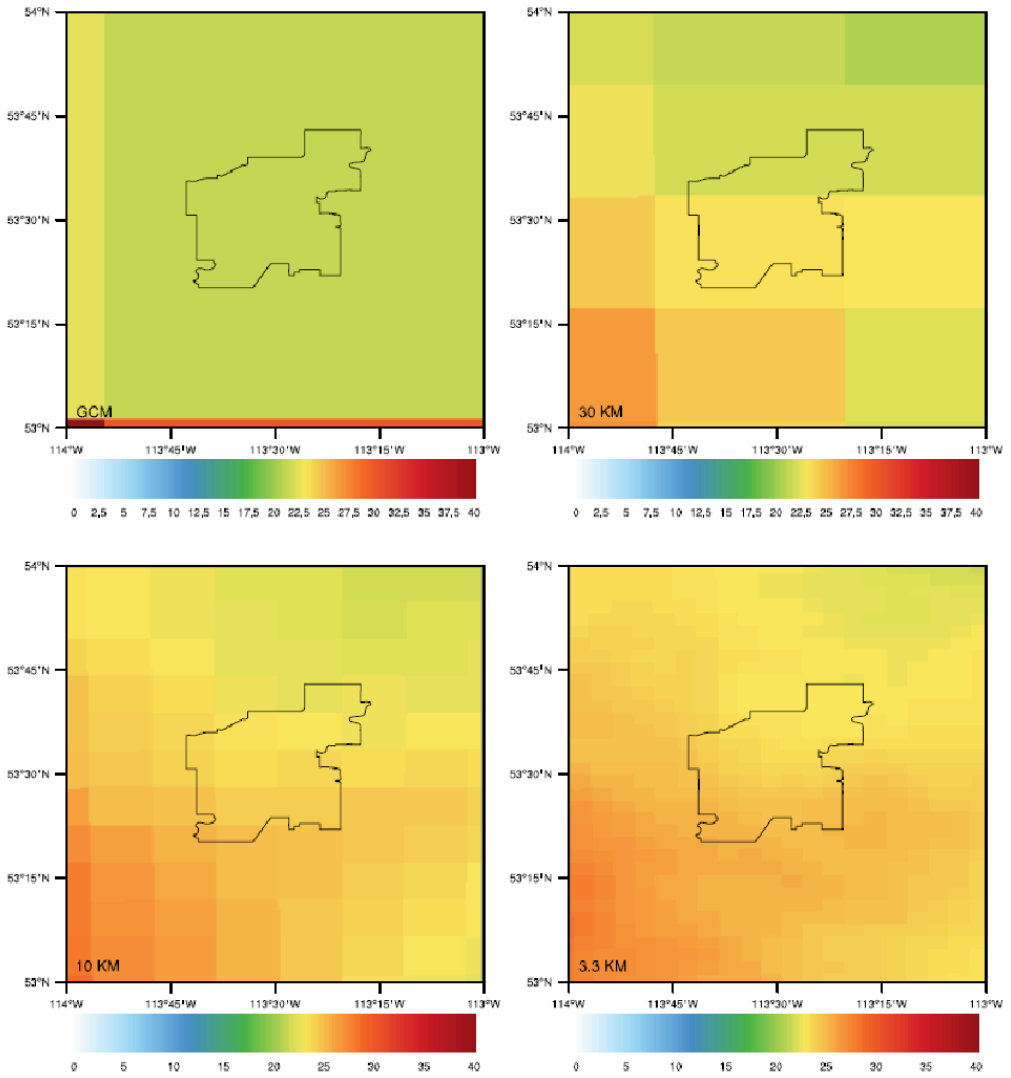

Figure 7: Model projections of the near future (2021-2050) total annual precipitation (cm) in the Edmonton region at four different spatial resolutions: GCM (> 110 km), and RCM domains at 30, 10 and 3.3 km resolution.

RCMs provide credible, physically based climate projections at the finer scales required for regional climate and impact studies. RCM experiments tend to be computationally demanding, depending on the domain size and resolution, and this has limited the length and number of many experiments. High-resolution (25 km) climate model data is available from the North American Domain of the Coordinated Regional Climate Downscaling Experiment (NA-CORDEX), a repository of daily data from the latest generation of Regional Climate Models (RCMs; Mearns et al., 2017). We also have access to a 15-member ensemble of bias-corrected data from

version 4 of the Canadian RCM (CanRCM4, RCP 8.5). The RCMs simulate the climate of the period 1950-2100 at various resolutions (25 km, 50 km, 0.22°, 0.44°) and for medium and high greenhouse gas emission scenarios (Representative Emission Pathways - RCPs 4.5 and 8.5). Our focus is two 30-year intervals: the near (2021-2050) and medium (2051-2080) future and RCP8.5. We used data from the ESM/RCM experiments listed in Table 2. This bias-corrected model output is available at a resolution of 25 km for a large set of climate variables.

Table 2: The 12 RCM experiments that were the source of the climate projections for this project. Each experiment pairs a RCM with an ESM. Eleven of the model experiments are from the NA-CORDEX. The 12th downscaling experiment (CESM-WRF; highlighted in red) was done for this study as described in detail below.

ESM	RCM
CanESM2	CanRCM4
CanESM2	CRCM5-UQAM
GEMatm-MPI	CRCM5-UQAM
GEMatm-Can	CRCM5-UQAM
GFDL-ESM2M	RegCM4
GFDL-ESM2M	WRF
HadGEM2-ES	WRF
MPI-ESM-LR	CRCM5-UQAM
MPI-ESM-LR	RegCM4
MPI-ESM-LR	WRF
MPI-ESM-MR	CRCM5-UQAM
CESM	WRF

Acronyms:

UQAM: University of Quebec at Montreal
GEMatm-MPI: Atmospheric Global Environment Model – Max Planck Institute version
GEMatm-Can: Atmospheric Global Environment Model – Canadian version
GFDL: Geophysical Fluid Dynamics Lab
RegCM4: Regional Climate Model (NCAR)
WRF: Weather Research and Forecasting Model
HadGEM2-ES: Hadley Centre Global Environment Model – Earth System
MPI-ESM: Max Planck Institute Earth System Model
LR: Low Resolution
MR: Mixed Resolution

3.1.1 The Weather Research and Forecasting (WRF) model

In addition to the RCM data available from NA-CORDEX, we generated climate projections for Edmonton at a resolution of 3.3 kilometers by utilizing the Weather Research and Forecasting (WRF) model version 4.0 (Skamarock et al., 2019). The US National Center for Atmospheric Research (NCAR) supports a worldwide community of WRF users by providing the code, documentation and tutorials. Our research team is registered with Compute Canada, which has enabled us to install and test the WRF model on a supercomputer in the WestGrid network (Basu et al., 2020). We are running WRF simulations forced with 6 hourly bias-corrected outputs from NCAR's Community Earth System Model (CESM1). We have configured the WRF model with nested horizontal grid resolutions of 30, 10 and 3.3 km. The 6-hourly model output includes a large set of climatic and hydrologic variables including temperature, pressure, humidity, precipitation, runoff, soil moisture, etc. We use the NCAR Command Language (NCL) on a local server for the post processing of the model output and for producing high quality graphics. We use 30-year intervals of sub-daily output for analyzing significant trends, extreme values, and the spatial distribution of various hydro-climatic parameters.

The National Center for Atmospheric Research (NCAR) Weather Research and Forecasting (WRF) model version 4.0 (Skamarock et al., 2019) is a mesoscale numerical weather prediction system suitable for atmospheric research and operational forecasting with a resolution of thousands of kilometers to a few meters. The WRF model offers a wide choice of physics and dynamical packages along with different parameterization options (Figure 8), which makes it widely used for regional climate studies.

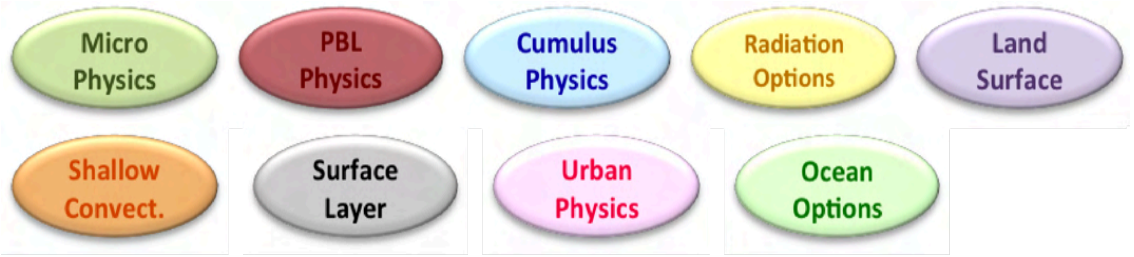

Figure 8: A chart showing different available parameterization schemes in WRF4.0

In this study, the WRF model was configured with 3 nested domains and a horizontal grid resolution of 30 km, 10 km and 3.3 km as shown in Figure 9. The model was setup as a 2-way nested domain run without any nudging in which all the domains were run simultaneously and communicate with each other. The nudging techniques relax the terms of the dynamical equations resulting in smoother values and hence it might result into under representation of the extreme values. The coarser domain provides boundary conditions to the finer resolution nested domain and the nested domain feeds its calculation back to the coarser domain. The highest-resolution domain primarily focuses on the city of Edmonton, whereas the 10 km domain captures the entire province of Alberta. The 30 km resolution domain covers a much

larger area, which includes almost the Prairie Provinces extending from the eastern slopes of the Canadian Rockies to western Ontario (Figure 9).

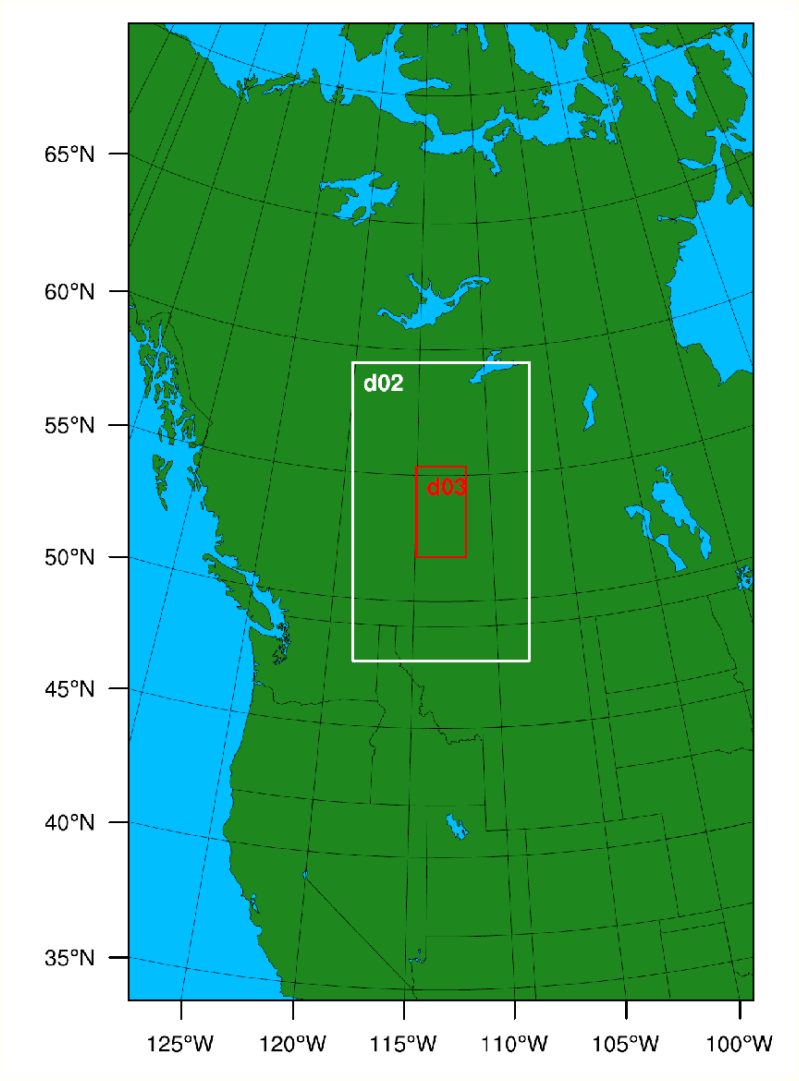

Figure 9: The nested domains of WRF simulation. The outer domain is the parent domain with a resolution of 30 km, d02 is the nested domain with a resolution of 10 km and d03 is the finest resolution nested domain with a resolution of 3.3 km.

In order to successfully initialize a WRF simulation, the pre-processing (WPS) component of the model requires a minimum set of meteorological and land-surface fields. The set of required fields is identified in Table 3.

Table 3: The set of meteorological and land-surface variables required fields to initialize a WRF simulation.

Variable	Units
3-d air temperature	K
3-d relative humidity	%
3-d specific humidity	kg kg^{-1}
3-d wind u-component	m s^{-1}
3-d wind v-component	m s^{-1}
3-d geopotential height	m
3-d pressure	Pa
Surface pressure	Pa
Mean sea-level pressure	Pa
Skin temperature	K
Soil height	m
2-meter air temperature	K
2-meter relative humidity	%
2-meter specific humidity	kg kg^{-1}
2-meter wind u-component	m s^{-1}
2-meter wind v-component	m s^{-1}
Land-sea mask (0=water, 1=land)	fraction
Soil moisture	m^3 m^{-3}
Soil temperature	K
Soil moisture	kg m^{-3}
Soil temperature	K

The model simulation was forced with global bias-corrected climate model output data from version 1 of NCAR's Community Earth System Model (CESM1; Monaghan et al., 2014) that was included in Phase 5 of the Coupled Model Intercomparison Experiment (CMIP5), which supported the Intergovernmental Panel on Climate Change Fifth Assessment Report (IPCC, 2013). The dataset contains all the variables needed for the initial and boundary conditions for simulations with the Weather Research and Forecasting model (WRF), provided in the Intermediate File Format specific to WRF. The data are interpolated to 26 pressure levels and are provided in files at six hourly intervals. The variables have been bias-corrected using the European Centre for Medium-Range Weather Forecasts (ECMWF) Interim Reanalysis (ERA-Interim) fields for 1981-2005, following the method in Bruyere et al. (2014). Files are available for a 20th Century simulation (1951-2005) and

Representative Concentration Pathway (RCP) future scenarios (RCP8.5) spanning 2006-2100.

WRF offers multiple physics options that can be combined in any way. The options typically range from simple and efficient, to sophisticated and more computationally costly, and from newly developed schemes to well-tried schemes such as those in current operational models. In this experiment the model physics configuration was:

- **Microphysics**
  WRF Single Moment class 6 (WSM6) Scheme: A scheme with ice, snow and graupel processes suitable for high-resolution simulations. (Hong and Lim, 2006)

- **Cumulus Parameterization**
  Kain Fritsch Scheme: Deep and shallow convection sub-grid scheme using a mass flux approach with downdrafts and CAPE removal time scale (Kain, 2004).

- **Longwave and Shortwave Radiation**
  RRTM (Rapid Radiative Transfer Model): It includes the MCICA method of random cloud overlap.

- **Planetary Boundary Layer**
  Mellor-Yamada-Janjic Scheme: One-dimensional prognostic turbulent kinetic energy scheme with local vertical mixing (2). (Nakanishi and Nino, 2009; Olson et al., 2019).

- **Surface Layer**
  Monin-Obukhov Scheme: Based on Monin-Obukhov with Zilitinkevich thermal roughness length (Janjic, 1996; 2001).

- **Land Surface**
  Unified NOAH Land Surface Model: A scheme with soil temperature and moisture in four layers, fractional snow cover and frozen soil physics. New modifications are added in Version 3.1 to better represent processes over ice sheets and snow covered area. (Tewari et al., 2004).

- **Cloud Fraction option**
  Xu-Randall Method. (Xu and Randall, 1996)

The model simulations were performed on the Compute Canada supercomputing platform using the academic supercomputer Cedar. The model runs generated 6-hourly outputs of more than 90 variables for the two finer resolution domains and daily output for the 30 km resolution domain. The simulation was performed for the historical period of 1st January 1975 to 31st December 2005; and for the near future period of 1st January 2021 to 31st December 2050; and far future period of 1st January 2051 to 31st December 2080.

3.2 RCM Projections of Annual and Seasonal Climate Changes

The conventional climate change scenario is the difference in the mean value of a temperature or precipitation variable between past and future 30-year periods. In Table 4, we compile the seasonal climate changes for the near (2021-2050) and far (2051-2080) future, relative to the 1976-2005 baseline, from the 11 ESM/RCM experiments plus the CESM-WRF simulation (30 km domain) run by PARC. Also given are the multi-model mean values. The largest changes in temperature are in winter and the least are in summer. The CESM-WRF projection of winter temperature change is the lowest among the RCMs but otherwise it gives results that are close to the mean values for the 12 ESM/RCM experiments. Winter also exhibits the largest increase in precipitation with the CESM-WRF simulation given among the highest values. This simulation is among those that project decreased precipitation in summer, although the multi-model mean indicates a marginal increase.

Table 4: Near (2021-2050) and Far (2051-2080) Future Projections of Seasonal Climate Changes from 11 ESM/RCM Experiments and the Multi-Model Mean Values

	Seasonal Precipitation Changes (%)							
	Winter		Spring		Summer		Fall	
	2021-2050	2051-2080	2021-2050	2051-2080	2021-2050	2051-2080	2021-2050	2051-2080
CanESM2-CanRCM4	-0.75	24.91	34.84	43.81	5.51	12.21	18.94	36.26
CanESM2-CRCM5	-7.04	9.82	40.74	53.58	-18.77	-23.66	23.03	22.81
GEMatm-MPI.CRCM5	11.72	9.89	19.18	19.70	-8.49	11.40	21.87	14.12
GEMatm-Can.CRCM5	1.74	12.17	12.93	31.01	1.94	9.01	6.70	6.91
GFDL-ESM2M.RegCM4	20.42	17.48	2.73	12.82	22.02	9.55	6.69	-3.71
GFDL-ESM2M.WRF	12.52	15.00	8.52	26.54	17.16	8.80	-3.99	-0.98
HadGEM2-ES.WRF	11.57	33.35	24.24	36.07	9.38	0.49	11.70	13.83
MPI-ESM_LR.CRCM5	18.86	14.50	-2.79	8.24	-4.69	3.45	22.41	11.04
MPI-ESM-LR.RegCM4	7.29	12.54	-6.48	22.54	28.16	18.33	17.11	14.51
MPI-ESM-LR.WRF	10.79	14.12	-9.85	0.05	-0.50	14.23	31.67	34.07
MPI-ESM-MR.CRCM5	7.29	9.76	-0.81	17.77	5.13	7.15	27.89	16.14
CESM-WRF	18.62	30.05	-3.33	0.94	-2.71	-4.07	-4.96	6.42
Ensemble Mean	**9.42**	**16.97**	**9.99**	**22.76**	**4.51**	**5.57**	**14.92**	**14.28**

	Seasonal Temperature Changes (^{0} C)							
	Winter		Spring		Summer		Fall	
	2021-2050	2051-2080	2021-2050	2051-2080	2021-2050	2051-2080	2021-2050	2051-2080
CanESM2-CanRCM4	3.84	4.91	2.33	3.05	2.68	5.25	1.77	4.63
CanESM2-CRCM5	4.13	5.20	2.82	3.46	2.99	-4.21	2.33	5.20
GEMatm-MPI.CRCM5	2.68	5.05	2.02	3.65	1.45	3.13	1.45	3.45
GEMatm-Can.CRCM5	3.71	5.70	3.03	3.25	2.06	3.84	2.40	4.69
GFDL-ESM2M.RegCM4	1.13	2.59	0.94	1.01	1.24	2.55	1.19	2.77
GFDL-ESM2M.WRF	1.85	3.77	2.52	3.04	1.20	2.40	1.73	3.45
HadGEM2-ES.WRF	3.62	6.69	2.79	4.19	1.59	4.81	2.59	5.91
MPI-ESM_LR.CRCM5	1.44	4.30	2.93	3.73	2.47	3.85	1.53	3.85
MPI-ESM-LR.RegCM4	1.63	5.25	2.33	3.18	1.81	3.40	1.19	3.64
MPI-ESM-LR.WRF	2.26	5.16	3.46	4.26	1.75	2.91	1.41	3.52
MPI-ESM-MR.CRCM5	2.30	4.72	2.67	3.69	2.31	3.73	1.15	3.34
CESM-WRF	1.62	2.53	2.18	3.11	1.51	3.22	1.74	3.56
Ensemble Mean	**2.52**	**4.66**	**2.50**	**3.30**	**1.92**	**2.91**	**1.71**	**4.00**

The seasonal climate changes listed in Table 4 can be visualized in Figures 10 and 11. These are scatter plots of the projected changes in total monthly precipitation (%) versus mean monthly temperature (^{0} C) for the near future (2021 to 2050) and far future (2051 to 2080) in comparison to the historical baseline period (1975 to 2005). The coloured dots represent the various ESM/RCM model simulations. The circled purple dot represents the WRF downscaling of the bias-corrected CESM data. The WRF projections fall within the spread of CORDEX data. The precipitation projections are above average for winter and below average for the other three seasons. The CESM-WRF temperature projections are below average in winter and near average for the other three seasons. Whereas all the model projections are equally probable, is it useful to know that the detailed CESM-WRF data generated for this project are not outliers in the larger distribution of model projections.

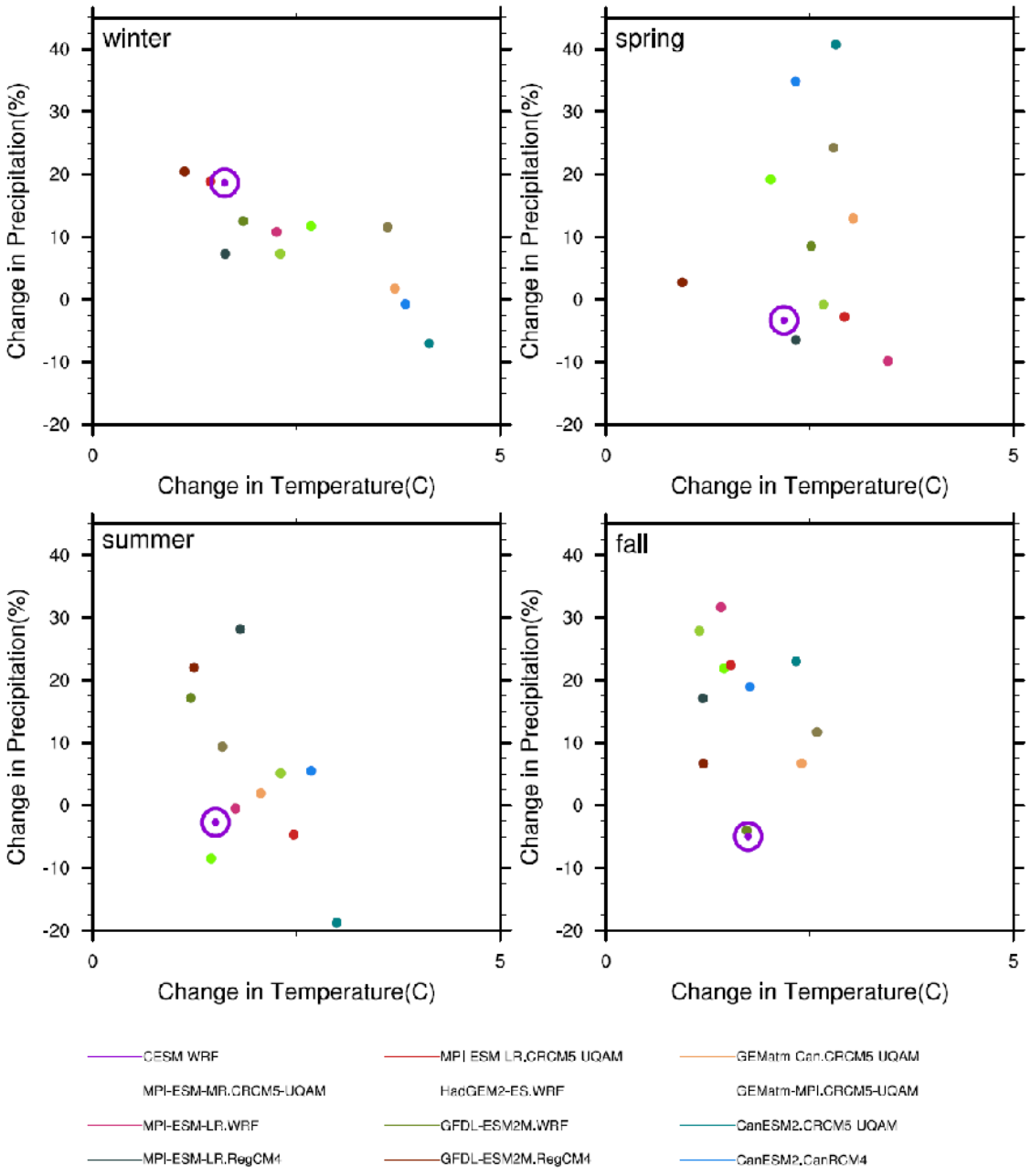

Figure 10: Scatter plots of projected changes in total monthly precipitation (%) and mean monthly temperature (^{0} C) in near future (2021 to 2050) in comparison to historical (1975 to 2005) in Edmonton (3.3 Km domain) for winter, spring, summer, and fall. The coloured dots represent different NA CORDEX models and the circled purple dot represents the WRF simulation using bias corrected CESM input data.

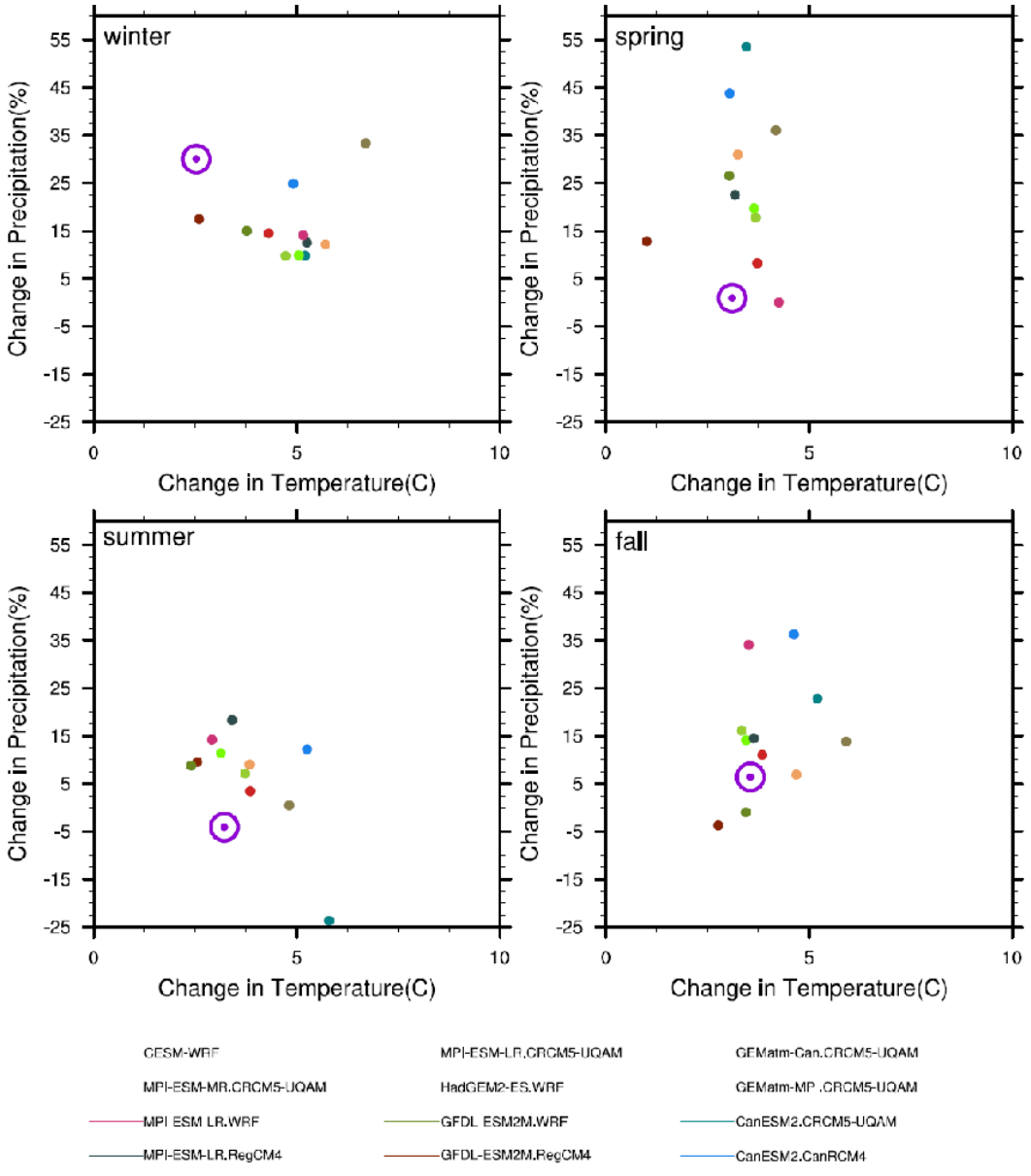

Figure 11: Scatter plots of projected changes in total monthly precipitation (%) and mean monthly temperature (^{0} C) in far future (2051 to 2080) in comparison to historical (1975 to 2005) in Edmonton (3.3 Km domain) for winter, spring, summer, and fall. The coloured dots represent different NA CORDEX models and the circled purple dot represents the WRF simulation using bias corrected CESM input data.

In Figure 12, multi-model mean seasonal precipitation and mean seasonal temperature are mapped using the data from the 11 CORDEX models for the historical (1976-2005), near future (2021-2050) and far future (2051-2080) periods. These maps illustrate the consistent increase in precipitation and temperature from the past to the future. At the 25 km resolution of the CORDEX RCMs, the climate is relatively

uniform across the Edmonton region, although the wetter conditions at higher elevation southwest of the City are evident in spring and summer. Also visible is a gradient in temperature from south to north. These distinctions with elevation and latitude do not appear at the coarse scale of global models; since the area mapped in Figure 10 and 11 corresponds to the approximate size of one GCM grid cell.

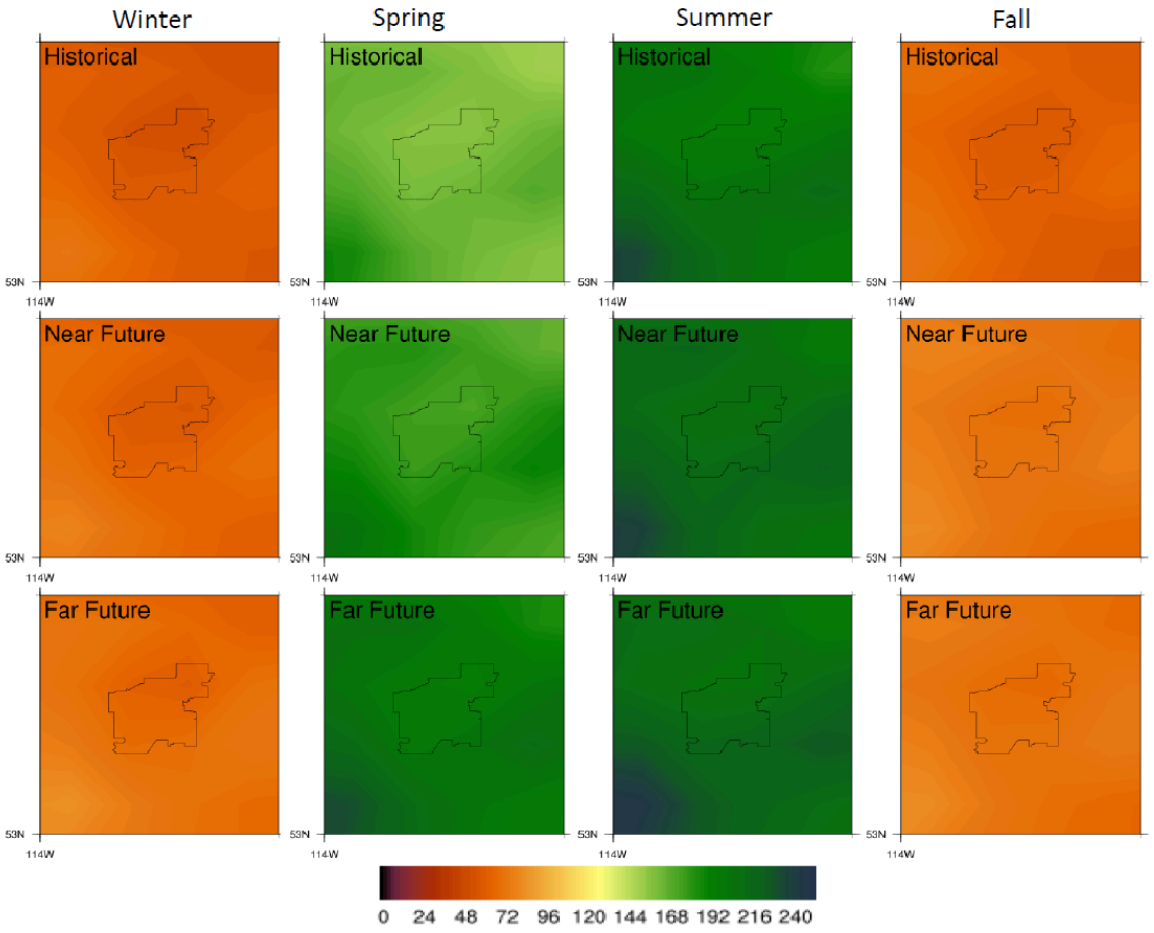

Figure 12: Multi-model mean seasonal total precipitation from 11 CORDEX models for the historical (1976-2005), near future (2021-2050) and far future (2051-2080) periods.

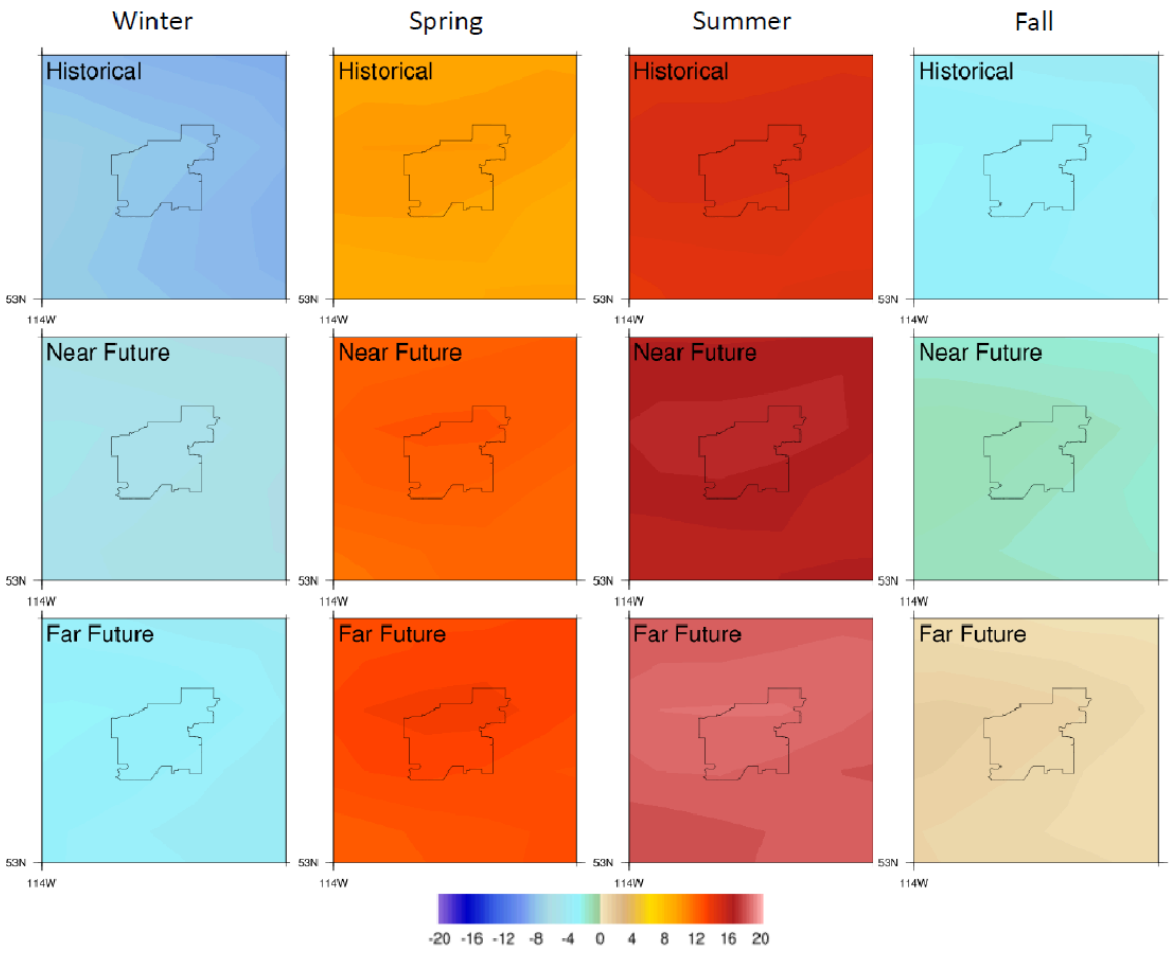

Figure 13: Multi-model mean seasonal temperature from 11 CORDEX models for the historical (1976-2005), near future (2021-2050) and far future (2051-2080) periods.

3.3 High-Resolution WRF Model Projections

Table 3 gave outputs from the WRF modeling at 30 km resolution in the form of shifts in mean seasonal temperature and precipitation. In this section of the report, we present the results from the high-resolution (3.3. km) WRF modeling in the form of time series plots and maps. Figures 14 and 15 are time series plots of projected mean annual temperature and precipitation from 2021 to 2080. Both variables are trending upwards, although the 60-year increase in precipitation (~ 20 mm) is small compared to the inter-annual range (~ 220 mm).

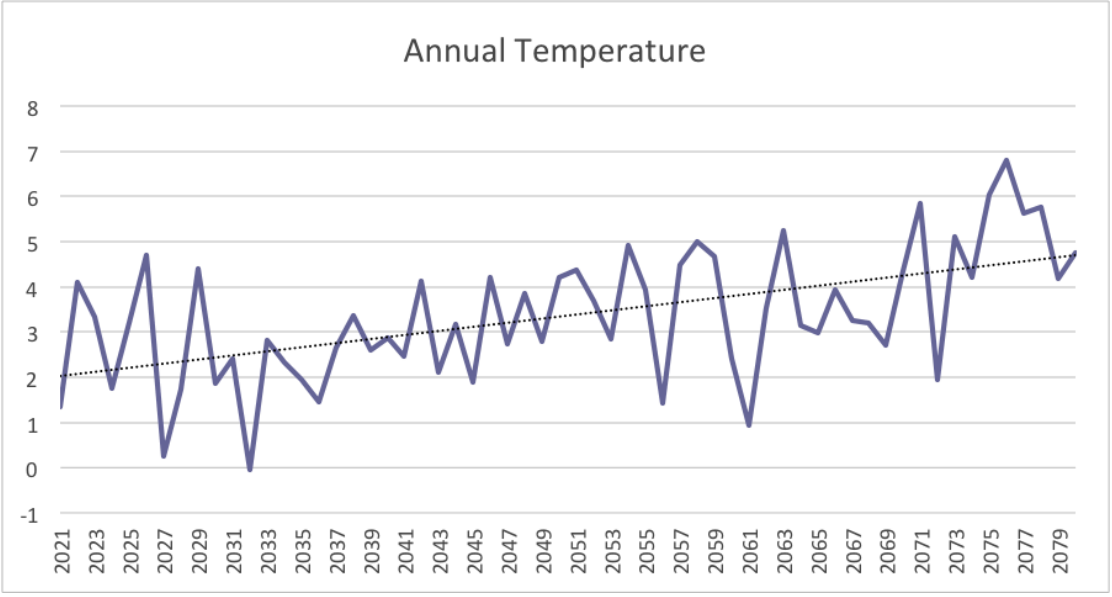

Figure 14: Time series of mean annual temperature (^{0} C) at Edmonton for the future (2021 to 2080) based on 3.3 km resolution WRF model outputs.

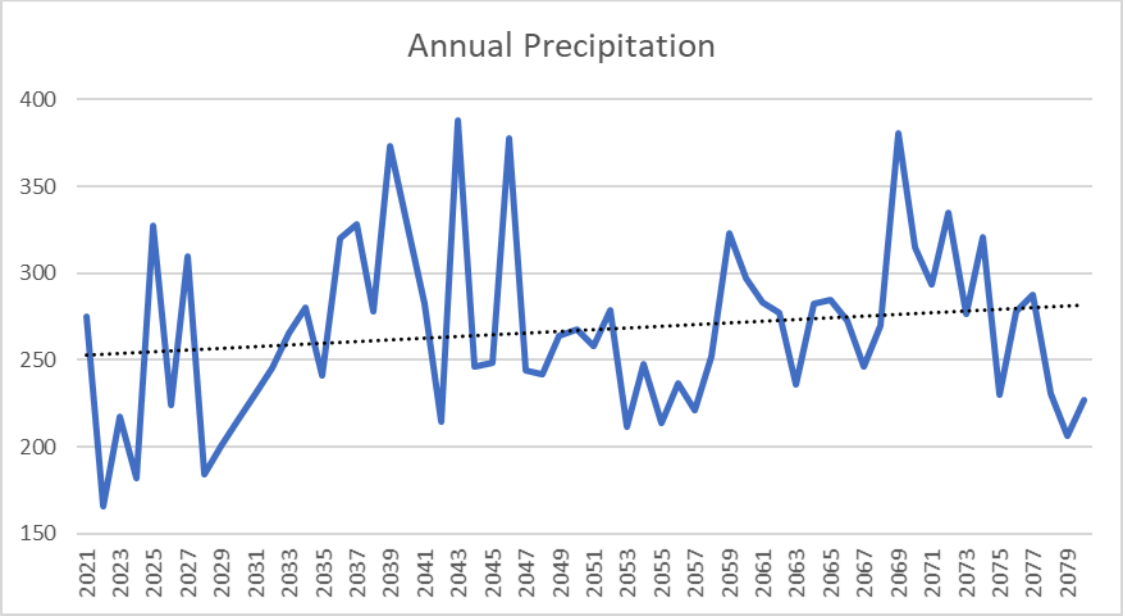

Figure 15: Time series of projected total annual precipitation at Edmonton in the future (2021 to 2080) calculated from 3.3 km WRF simulations.

In Figure 16, the time series of seasonal mean temperature (^{0} C) from 2021 to 2080 indicates a highest increase in summer and fall (3.6 ^{0} C), although the other seasons are not far behind. Figures 17 and 18 are time series plots of mean daily minimum winter temperature and mean daily maximum summer temperature, showing significant upward trends in both variables.

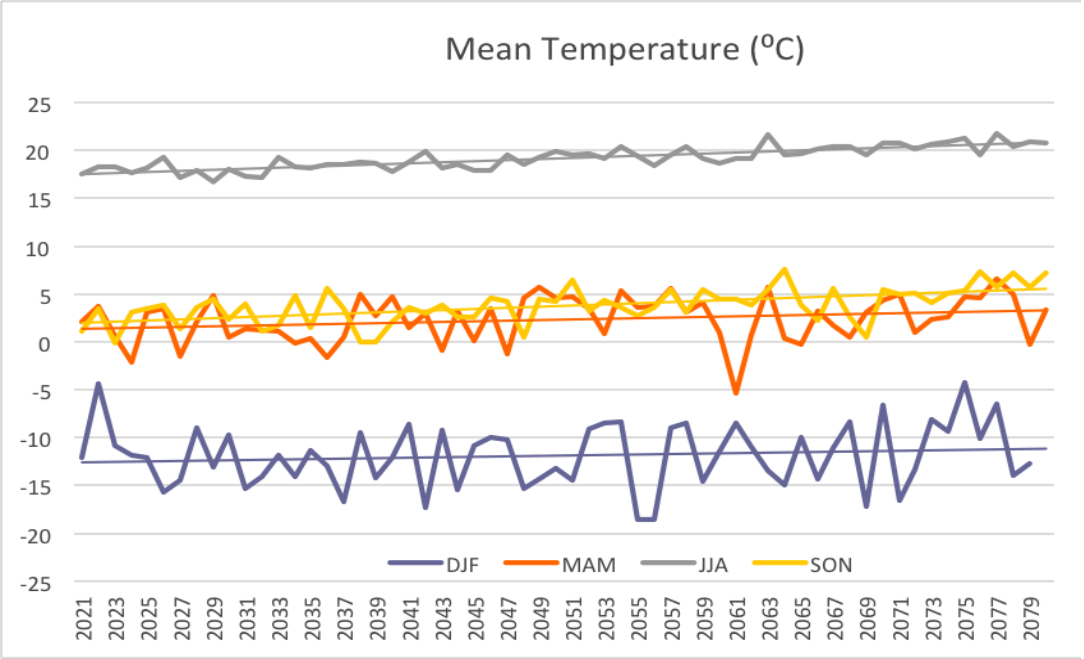

Figure 16: Time series of seasonal mean temperature (^{0} C) at Edmonton from 2021 to 2080. The highest increase in mean temperature is in summer and fall (3.6 ^{0} C)

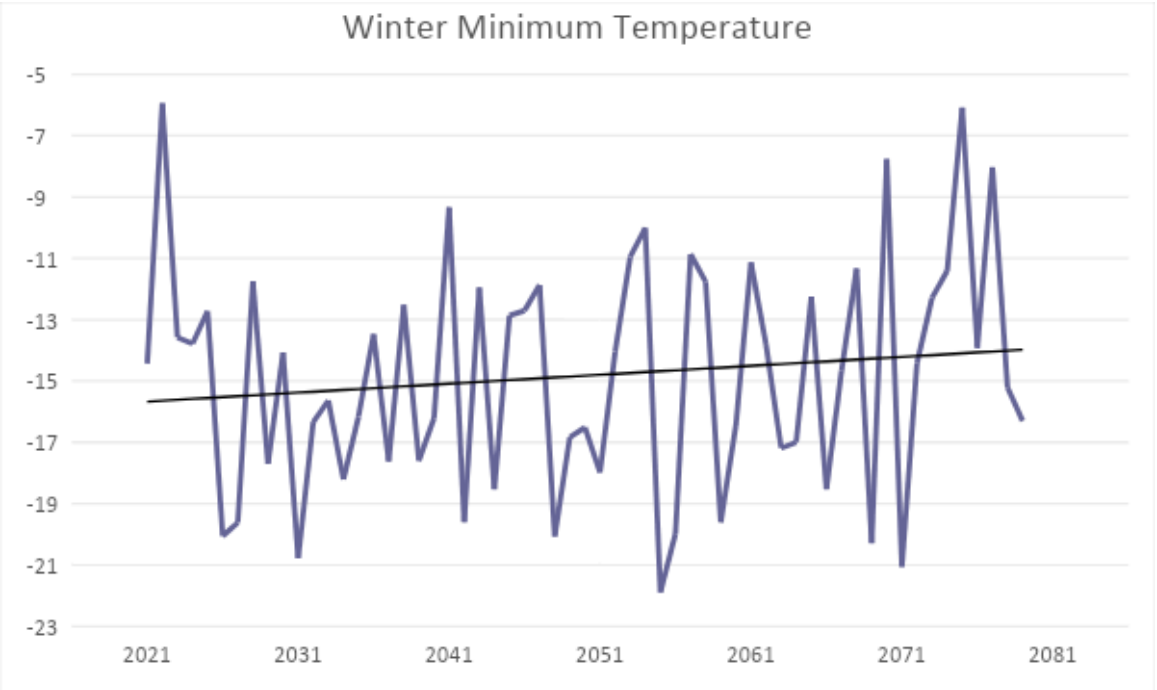

Figure 17: Time series of mean daily minimum winter temperature (^{0} C) at Edmonton for the future (2021 to 2080) based on 3.3 km resolution WRF model outputs.

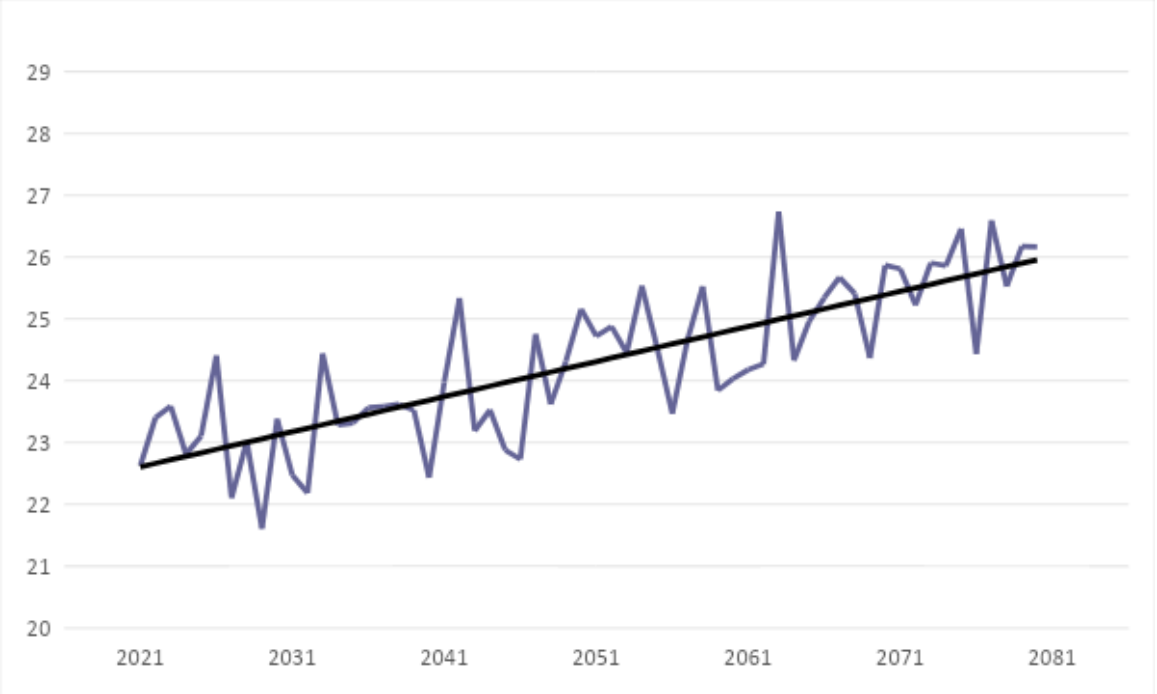

Figure 18: Time series of Mean Daily Summer Maximum temperature (^{0} C) of Edmonton for the future (2021 to 2080) based on 3.3 Km resolution WRF model outputs.

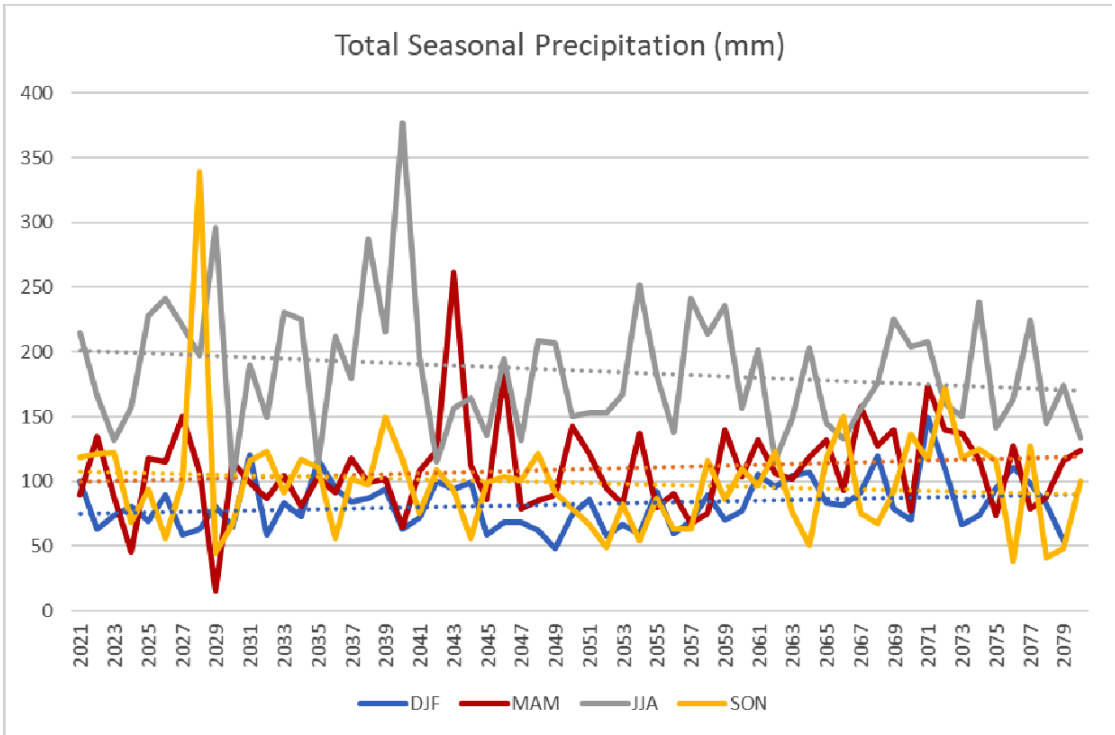

Figure 19: Time series of total seasonal precipitation (mm) at Edmonton. The largest long-term decrease and increase in total mean precipitation are in summer (- 30.6 mm) and spring (19.8 mm), respectively.

While the time series plots illustrate the climate trends and year-to-year variability, the major advantage of the WRF modeling is the high spatial resolution. To illustrate this point, Figure 20 has maps displaying the change in near future (2021-2050) and far future (2051-2080) total annual precipitation (mm) from the historical (1975-2005) baseline climate. Geographic details are very noticeable. In the near future, precipitation in the EMR and an area to the north is mostly unchanged or slightly decreased while elsewhere precipitation has begun to increase. In the far future, precipitation is higher throughout the region, with the least increase on the City's south side and to the southwest of the City.

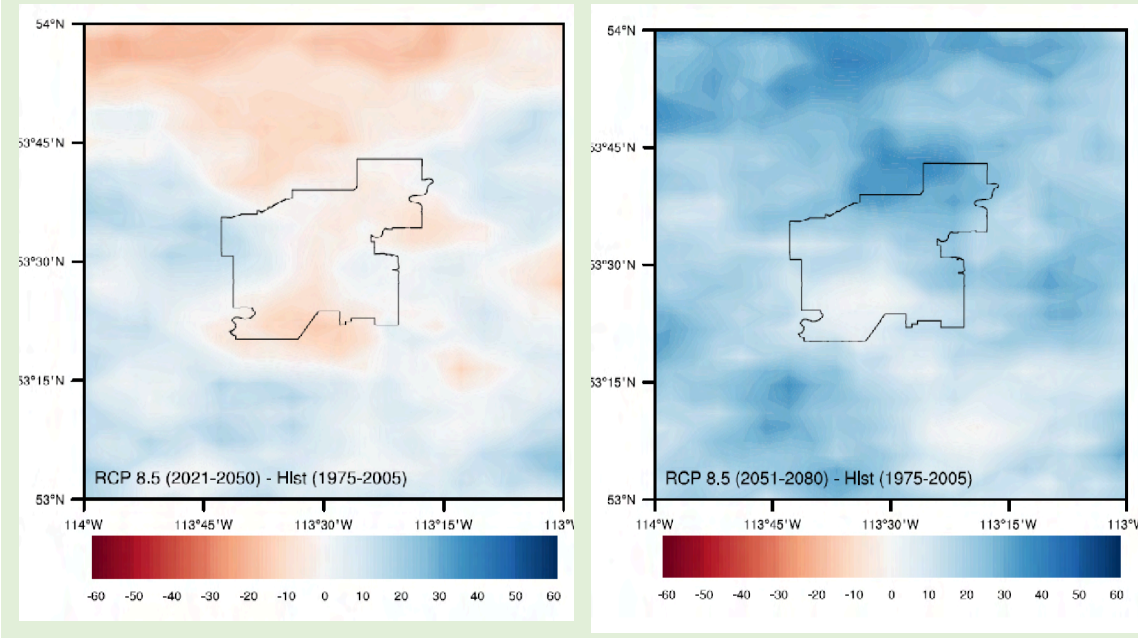

Figure 20: Difference in total annual precipitation (mm) in the near future (2021 to 2050) and far future (2051 to 2080) in comparison to historical (1975 to 2005) baseline climate.

Figures 21 and 22 consist of maps of the near and far future changes in monthly mean precipitation. These maps show increased precipitation in some months and decreases in other, although in general the warm months are drier and the cold months tend towards wetter as they become less cold. Again the high spatial resolution is evident in the differences among the 3.3 km grid cells and distinctions in climate change within the City limits. In some months (i.e., July and November) there is a contrast in the direction and magnitude of change between the near and far future. This reflects a large component of natural variability in the hydroclimate of Alberta. The regional signal of global climate change is embedded in this inter-annual and decadal variability. This influence of natural variability on the projection of future climate is the theme of the concluding section of this report.

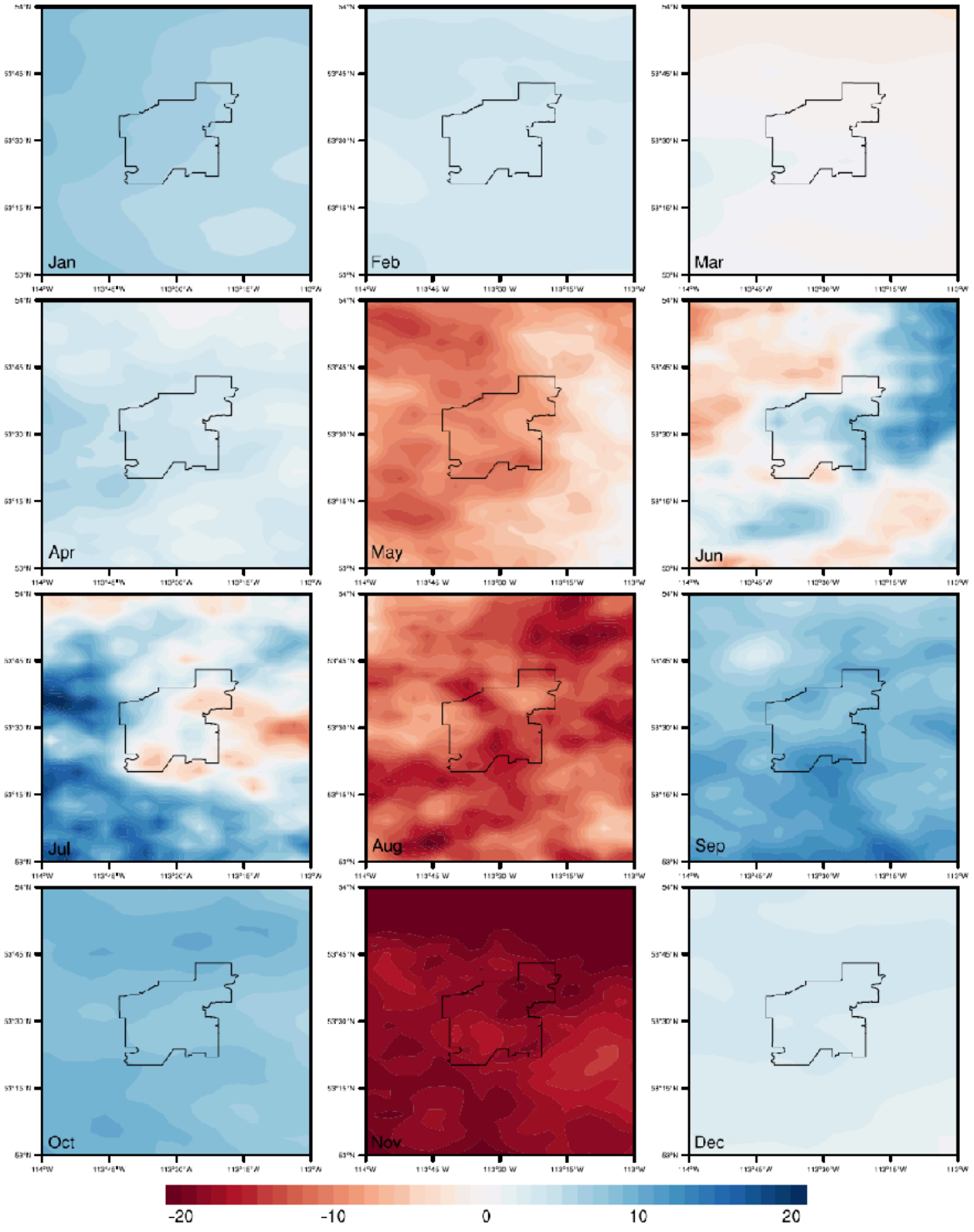

Figure 21: Changes in monthly mean precipitation (mm) in each month in the near future (2021-2050).

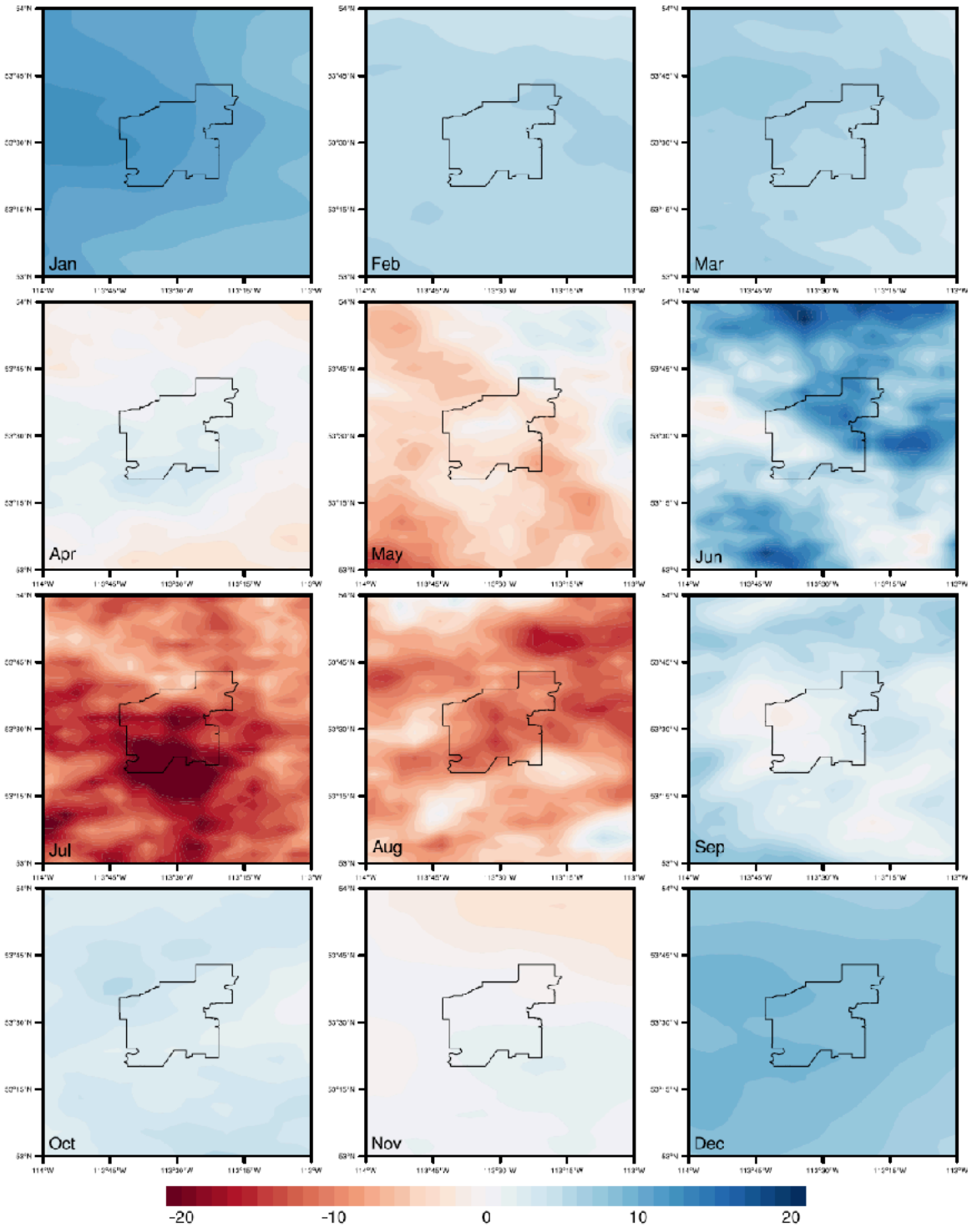

Figure 22: Changes in Long Term Monthly Mean Precipitation (mm) in each month in the far future (2051-2080).

Figures 23 and 24 consist of maps of the near and far future changes in monthly mean temperature (^{0} C). Temperature is more spatially homogenous then precipitation. Even

so, spatial gradients are apparent, particularly in spring. Temperatures increase in all months throughout the region, although in winter and spring there is a gradient from lower to higher rates of change from the southwestern to northeastern parts of the region. As with precipitation, contrasts between months and the near / far future periods reflects natural decadal-scale variability that can obscure the regional signal of global climate change.

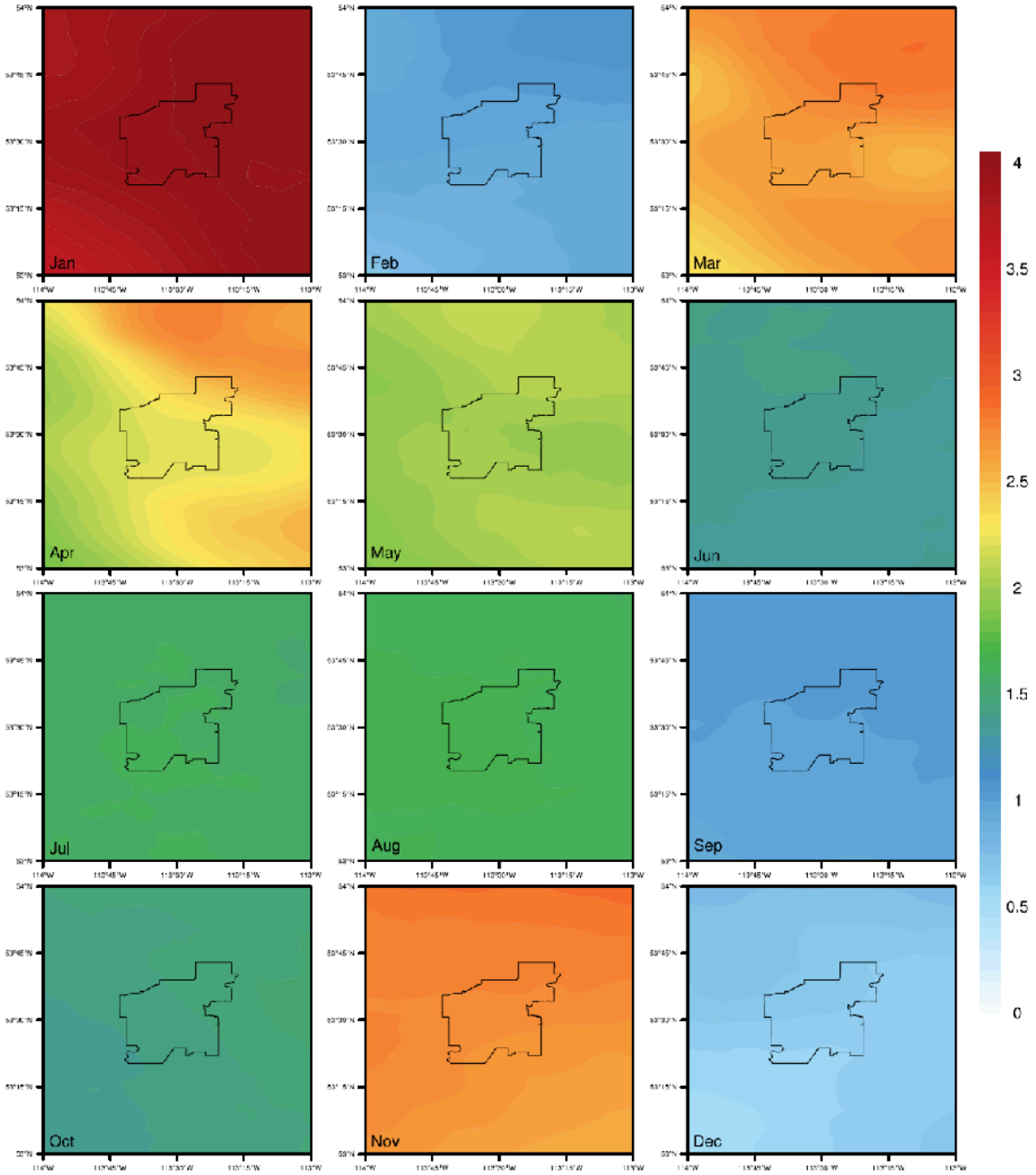

Figure 23: Changes in monthly mean temperature (^{0} C) in the near future (2021-2050).

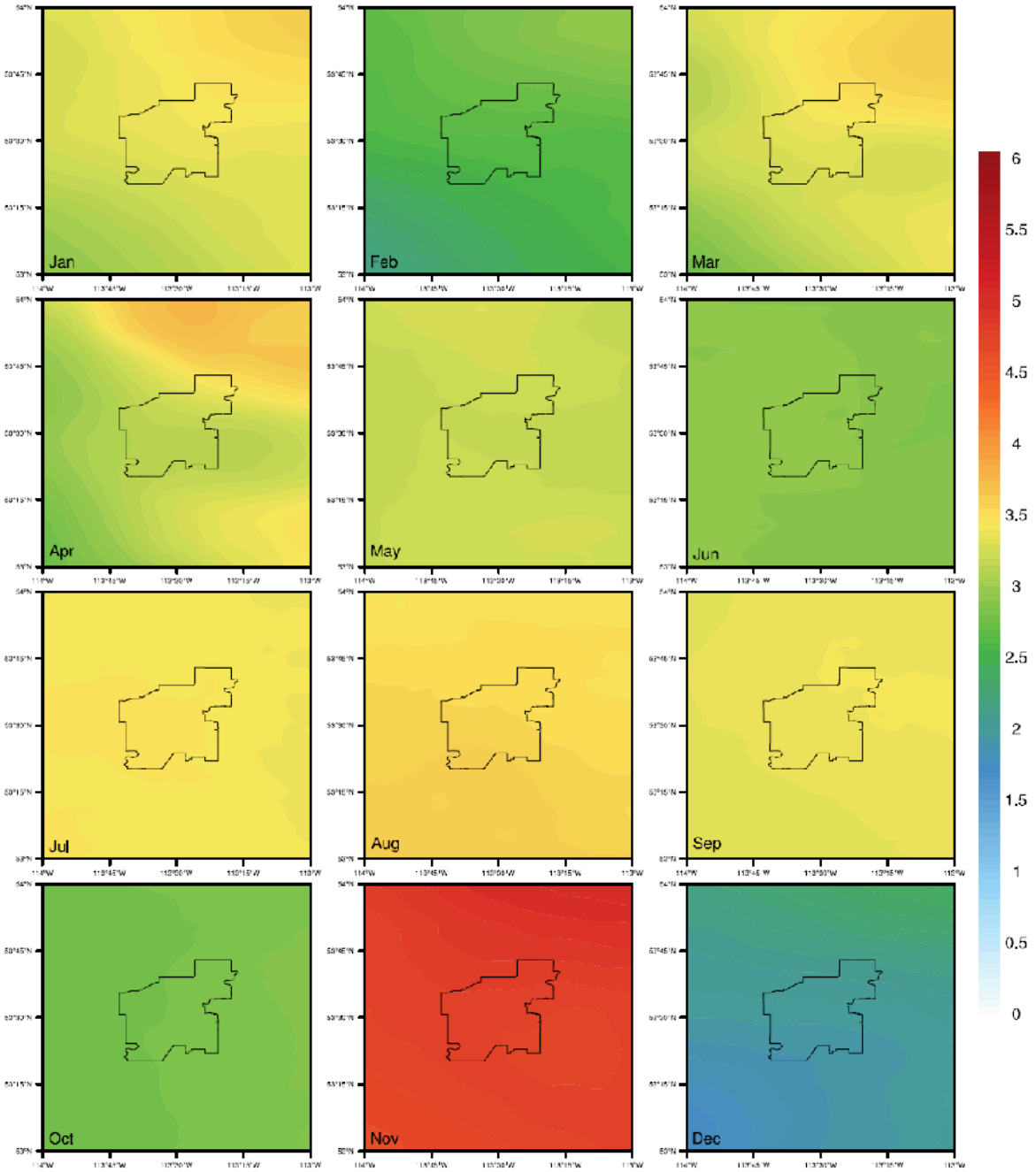

Figure 24: Changes in monthly mean temperature (^{0} C) in the far future (2051-2080).

With the high (sub-daily) temporal resolution of the WRF modeling, we were able to develop projections of climate extremes. Figures 26 and 27 are maps of the near and far future counts and changes in the number of wet (precipitation ≥ 5 mm) and very wet (precipitation ≥ 10 mm) days. The top 3 maps in both Figures show an increase in the absolute number of days going forward, with the southwest to northeast gradient that appears in many of the maps of WRF 3.3 km output. The bottom 2 maps in both

Figures show near and far future increases of up to 4 more days of wet and very wet days, although with much spatial variability. There are even small areas of no change or a slightly decreased frequency of very wet days.

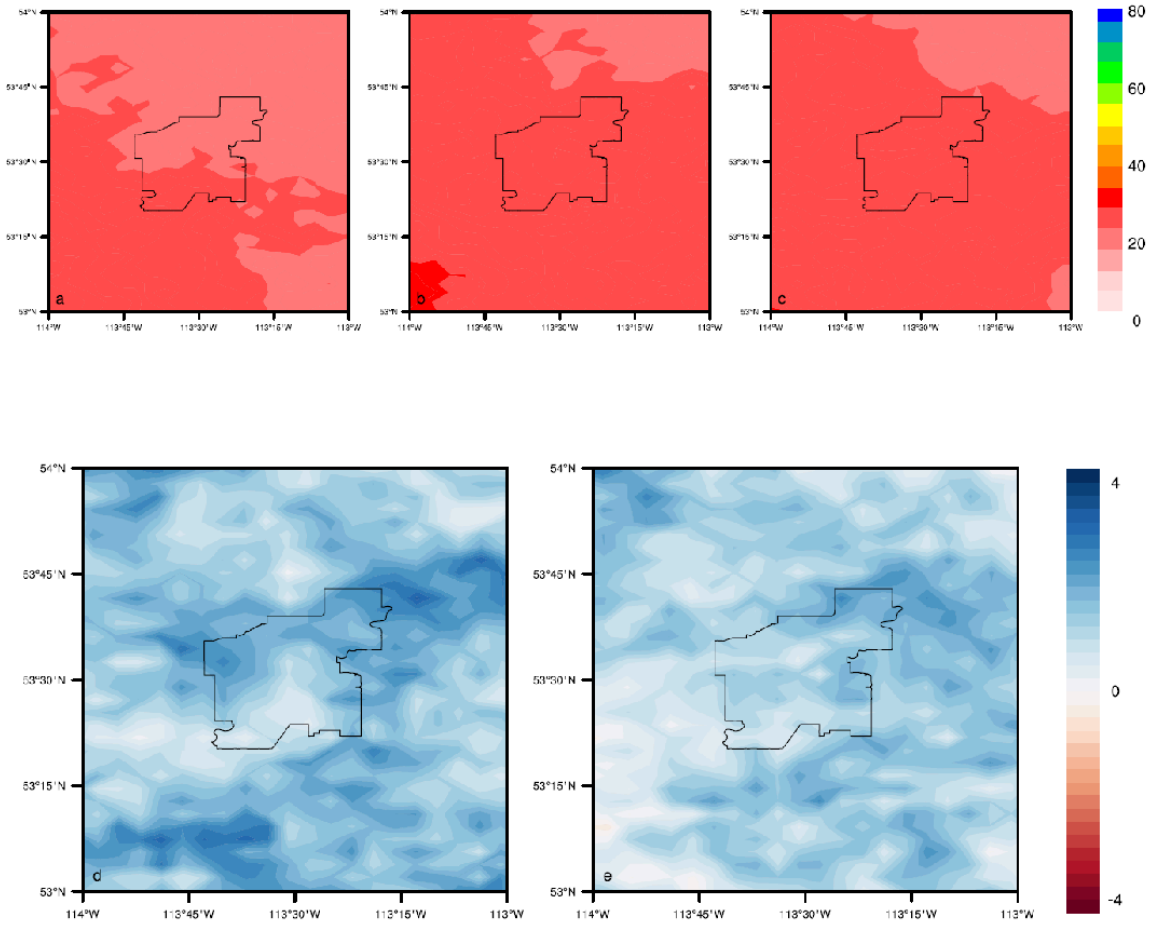

Figure 25: Number of wet days (precipitation ≥ 5 mm. a) Historical (1975 to 2005), b) Near Future (2021 to 2050), c) Far Future (2051 to 2080), d) Difference Near Future – Historical, e) Difference Far Future – Historical.

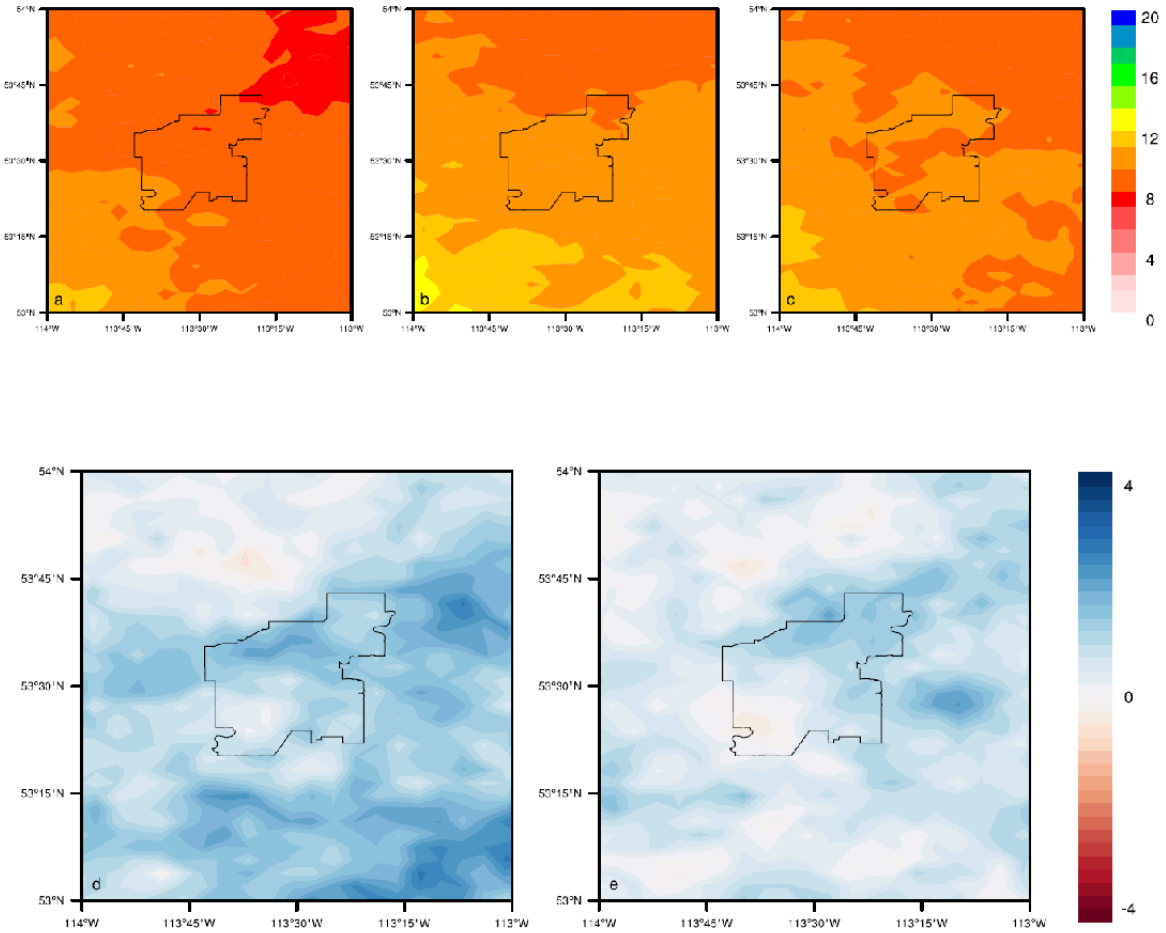

Figure 26: Number of very wet days (precipitation ≥10 mm). a) Historical (1975 to 2005), b) Near Future (2021 to 2050), c) Far Future (2051 to 2080), d) Difference Near Future – Historical, e) Difference Far Future – Historical.

The number of dry days (precipitation ≤ 1 mm) in Figure 27 increases going forward although not to the extent of wet days (note the different scales in Figures 25 and 27). The climate change maps in Figure 27 show that the number of dry days declines from the historical climate (1975-2005) to the climate of near (2021-2050) future and then increases into the far future (2051-2080). Again this is very likely a function of the natural inter-annual and decadal variability of Alberta's climate. There is considerable spatial variably in Figure 27, with far future decreases in number of dry days to the west of Edmonton and increases elsewhere in the region.

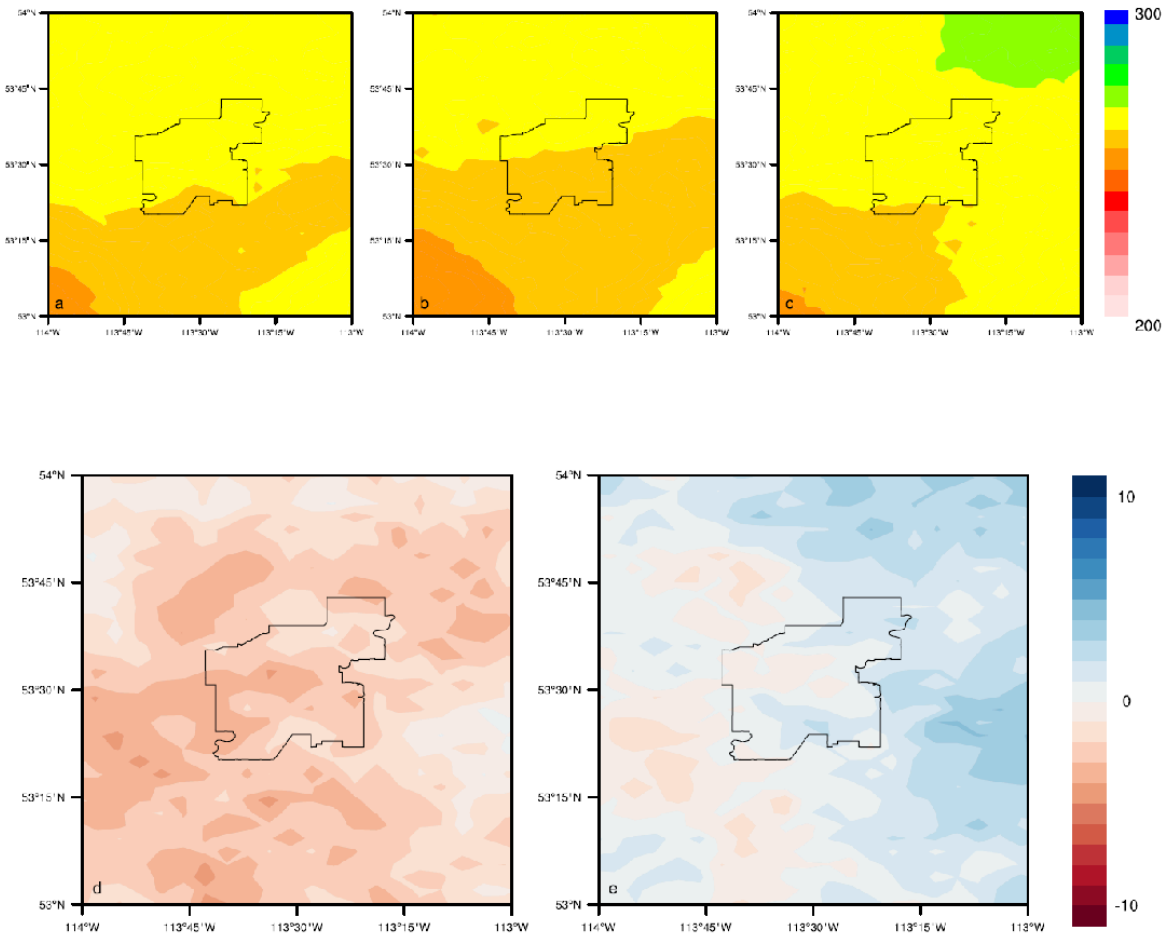

Figure 27: Number of dry days (precipitation ≤ 1 mm). a) Historical (1975 to 2005), b) Near Future (2021 to 2050), c) Far Future (2051 to 2080), d) Difference Near Future – Historical, e) Difference Far Future – Historical.

In Figures 28 and 29, the number of hot and very hot days (maximum temperature ≥ 30^0 and ≥ 35^0 C, respectively) increases markedly into the future, with the largest increases concentrated within the City limits.

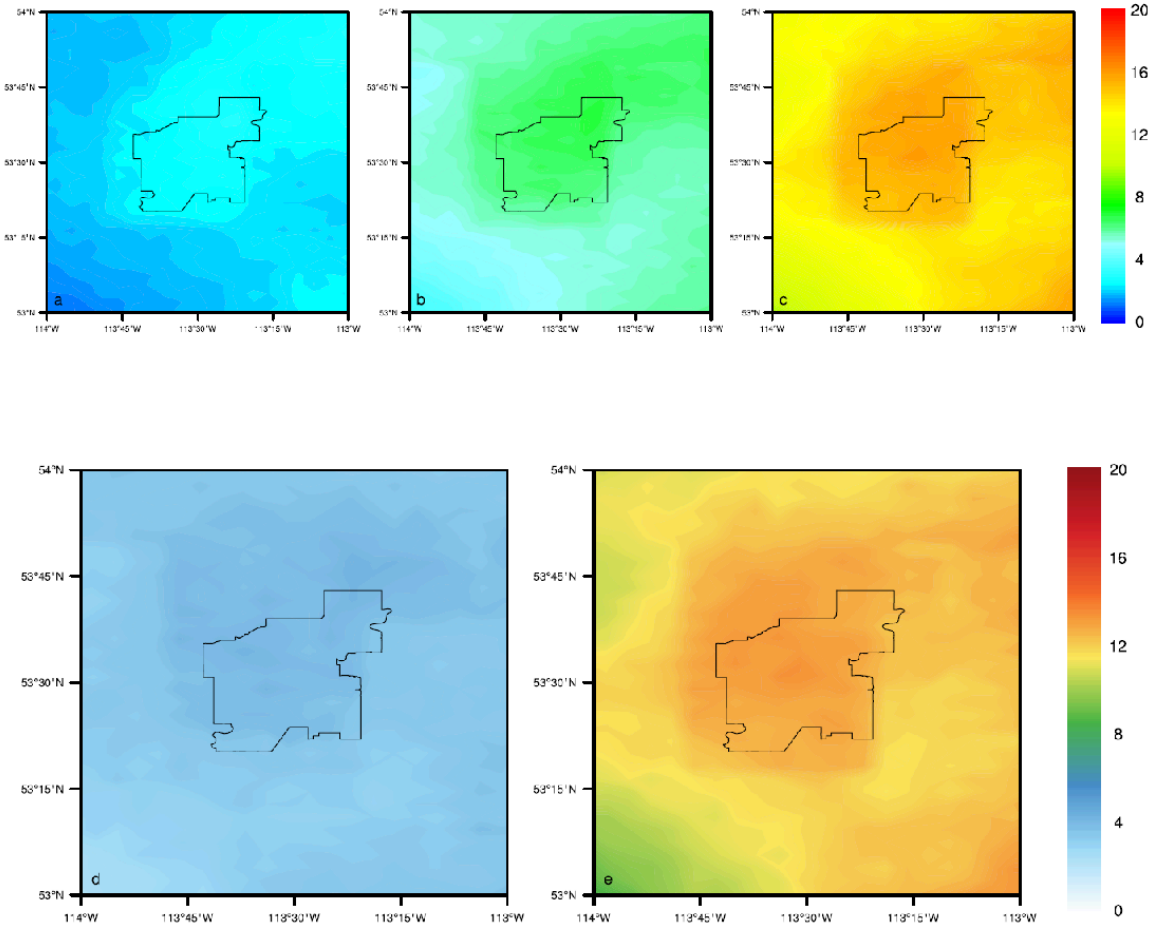

Figure 28: Number of hot days (maximum temperature ≥ 30^{0}C) . a) Historical (1975 to 2005), b) Near Future (2021 to 2050), c) Far Future (2051 to 2080), d) Difference Near Future – Historical, e) Difference Far Future – Historical.

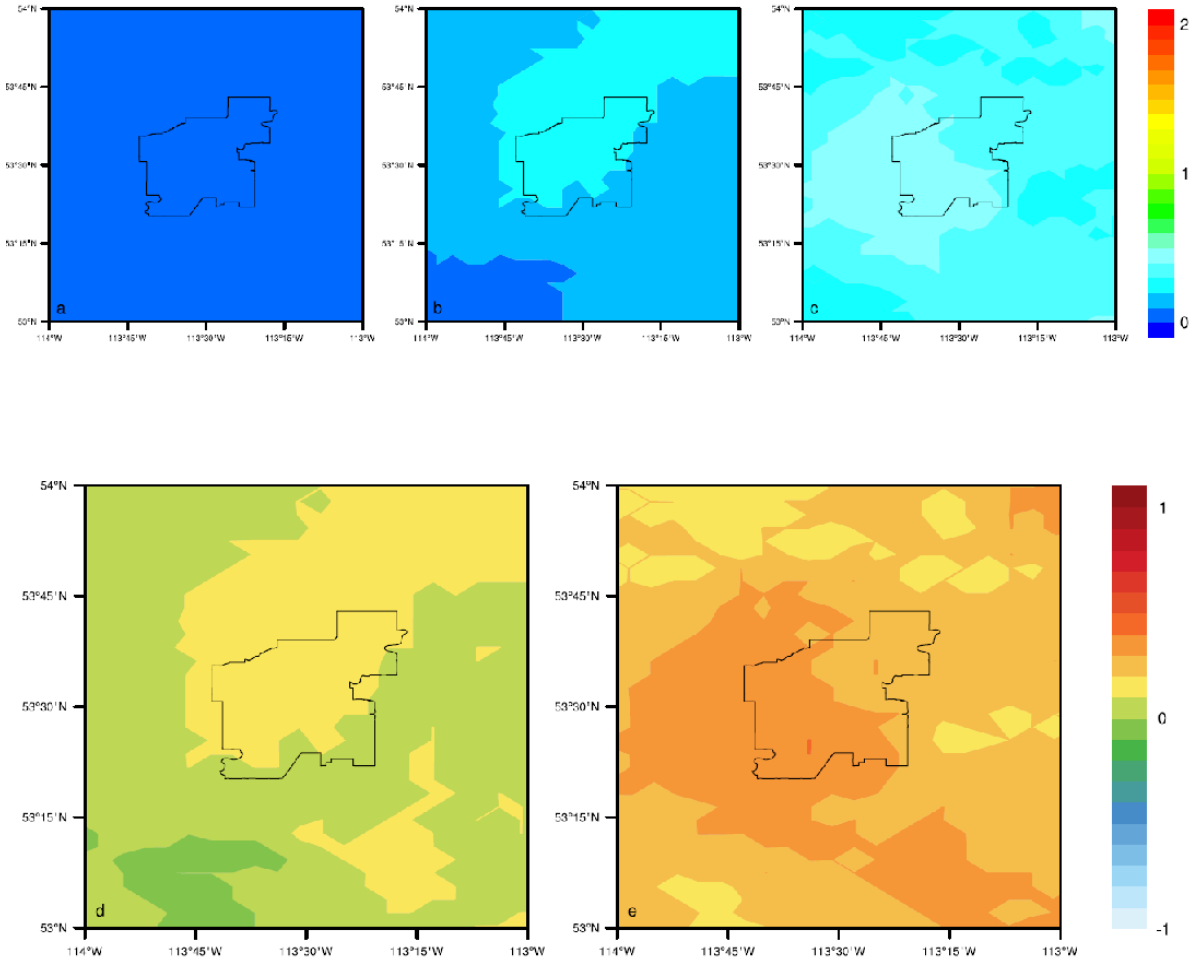

Figure 29: Number of very hot days (maximum temperature ≥ 35^{0}C) . a) Historical (1975 to 2005), b) Near Future (2021 to 2050), c) Far Future (2051 to 2080), d) Difference Near Future – Historical, e) Difference Far Future – Historical

The final set of maps from the WRF 3.3 km simulations show the number of moderate cold and very cold days (minimum temperature ≤ -10^0 C and ≤ -20^0 C, respectively) in Figures 30 and 31. The changes are dramatic with up to 30 fewer cold days and 20 fewer very cold days. There is an obvious spatial gradient from southwest to northeast.

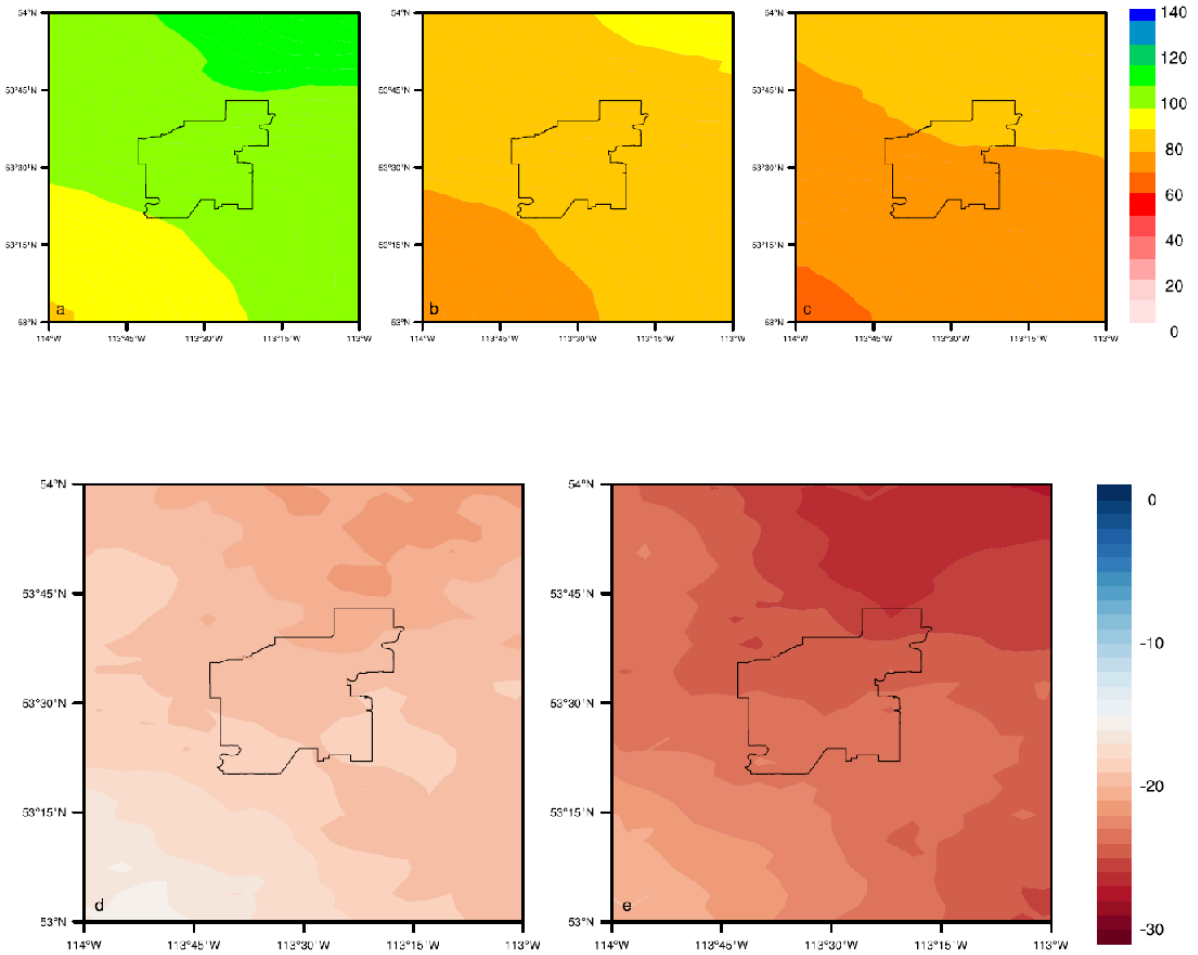

Figure 30: Number of moderate cold days (minimum temperature ≤ -10^{0}C) . a) Historical (1975 to 2005), b) Near Future (2021 to 2050), c) Far Future (2051 to 2080), d) Difference Near Future – Historical, e) Difference Far Future – Historical

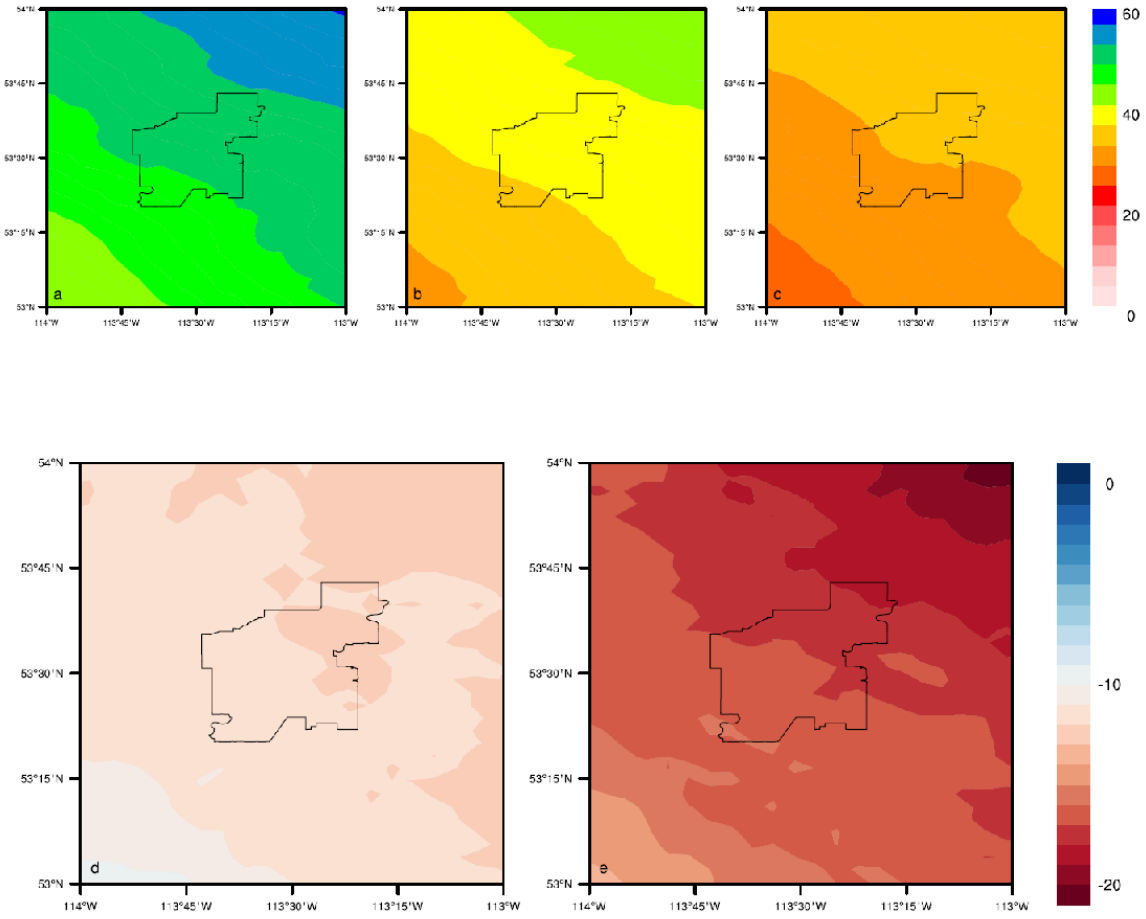

Figure 31: Number of very cold days (minimum temperature ≤ -20^0 C) . a) Historical (1975 to 2005), b) Near Future (2021 to 2050), c) Far Future (2051 to 2080), d) Difference Near Future – Historical, e) Difference Far Future – Historical

4 Extreme Precipitation and Runoff

A major advantage of the higher resolution of RCMs is the improved modeling of precipitation and extreme climate. We exploited this advantage with the 3.3 km WRF modeling as illustrated above in Figures 25 to 31 of the changes in the frequency of wet / dry and hot / cold days above and below specific thresholds. We further explored changes in daily precipitation using another approach that also enables us to study runoff and river levels and address the important issue of causes of uncertainty in the projection of the future climate of the EMR.

For this aspect of the project, we used data from only one of the NA-CORDEX models: version 4 of the Canadian Regional Climate Model, because we were able to access an ensemble of 15 runs of CanRCM4 (RCP8.5). Figure 32 is a scatterplot of the 15 simulations of temperature (° C) and precipitation (%) change from the ensemble of initial-condition CanRCM4 (RCP8.5) simulations. The range of future

temperature and precipitation is similar between this scatterplot and those in Figures 10 and 11 based on the 11 different NA-CORDEX RCMs. However, whereas the spread of projected climate changes in Figures 10 and 11 represents uncertainty resulting from the use of different climate models, the range of climate change projections in Figure 32 reflects different initial conditions as a function of the internal variability of the climate system. Thus we are able to explore the influence of two sources of uncertainty of the projection of future climate: the models and internal natural variability of the regional climate regime. We discuss this uncertainty in the Discussion section of this report. Here we present the daily precipitation projections from the ensemble of CanRCM4 simulations.

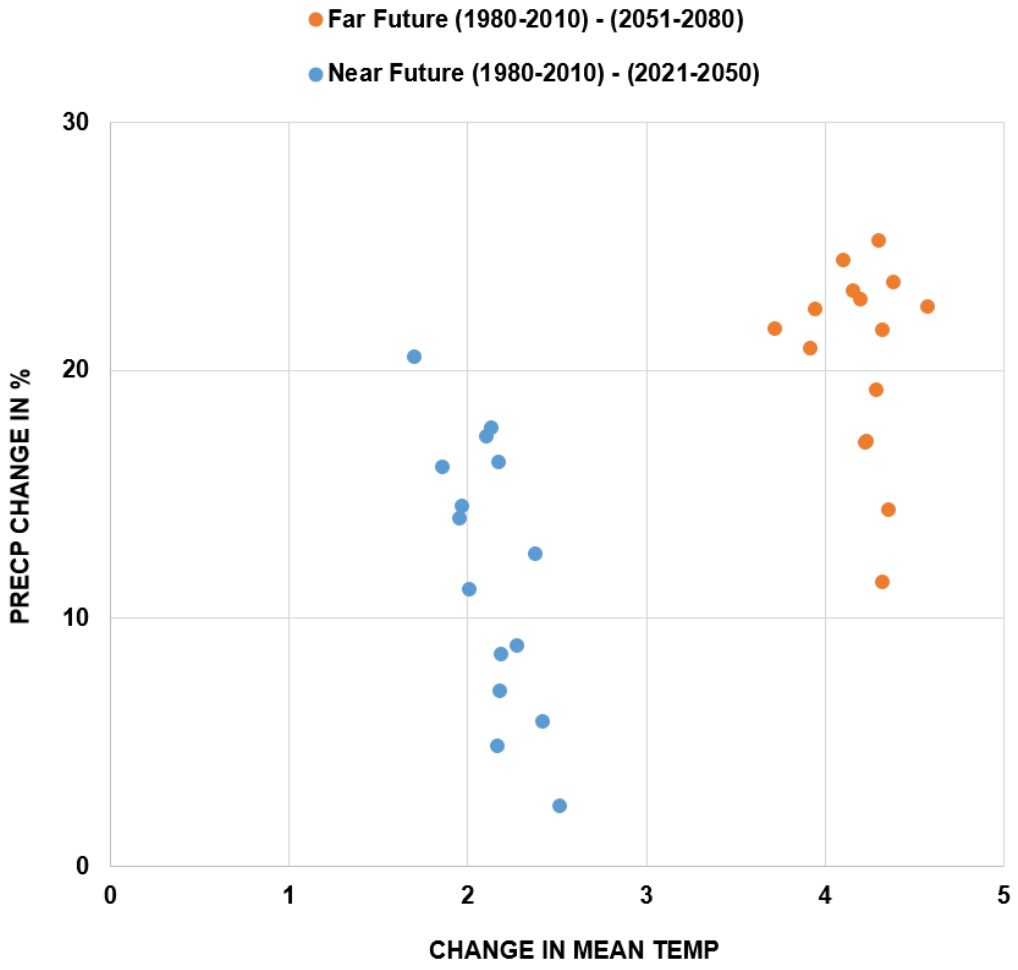

Figure 32: Scatterplot of mean temperature (° C) and precipitation change (%) at Edmonton. These climate projections are from a 15-member ensemble of initial-condition simulations from CanRCM4 (RCP8.5).

The time series of maximum daily precipitation (mm/day) in Figure 33 shows a significant rise from 1951 to 2100. Since these data are from a single model (CanRCM4), and based one GHG emission scenario (RCP8.5), differences among the 15 curves represent the natural internal variability of the climate of the Edmonton

region (the NSRB above the City). As important as a rise in the mean value is the increased frequency of extreme daily precipitation exceeding 300 mm in one day.

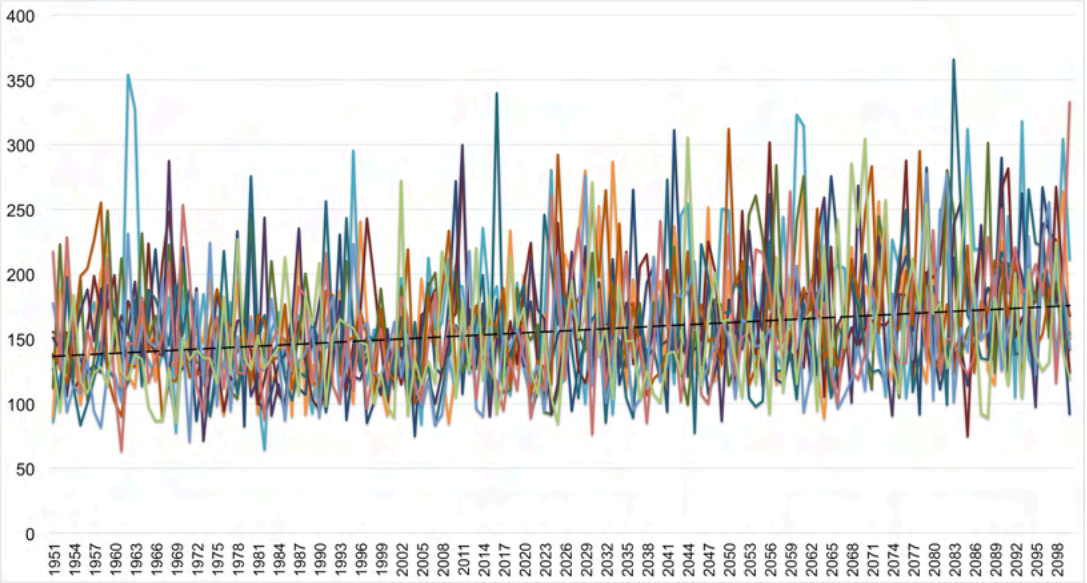

Figure 33: Maximum daily precipitation (mm/day) in the NSRB above Edmonton from an ensemble of CanRCM4 initial-conditions projections.

Figures 34 to 37 are time series of the frequency of days above and below a 1 mm precipitation threshold. The number of wet days (> 1 mm) and the length of wet spells (consecutive days) both display upward trends, with some long wet spells in the future. While the number of wet days, and length of wet spells, might seem large; the model records a wet day when precipitation of more than 1 mm occurs at any location (25 km grid cell) in NSRB above Edmonton. In Figure 36, there is a strong downward trend in the number of dry days (< 1 mm) per year and a lesser decline in the length of dry spells.

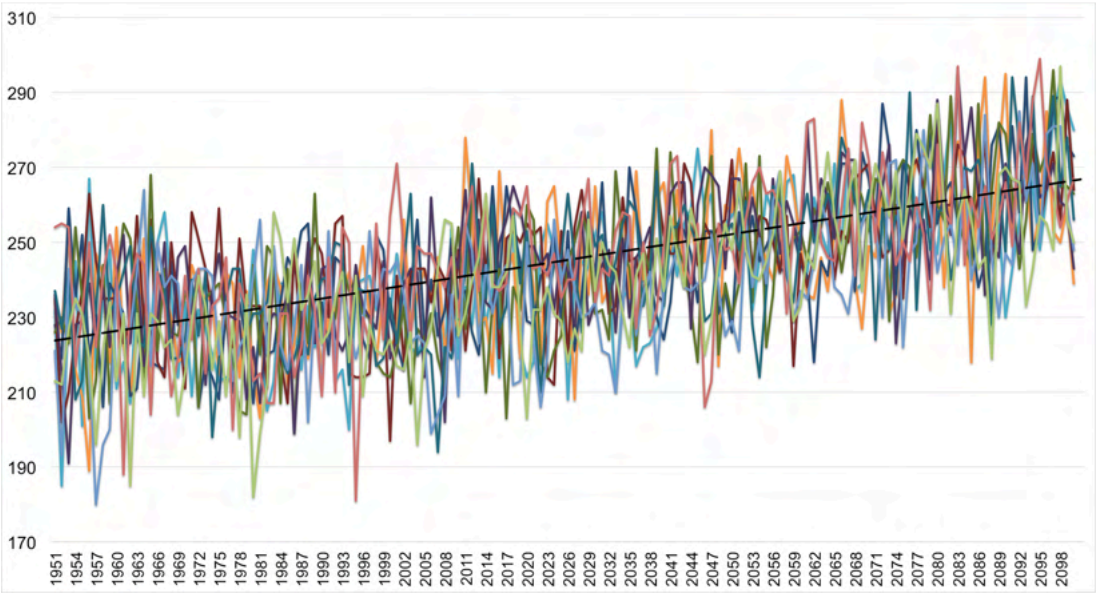

Figure 34: Number of wet days (> 1 mm) per year in the NSRB above Edmonton.

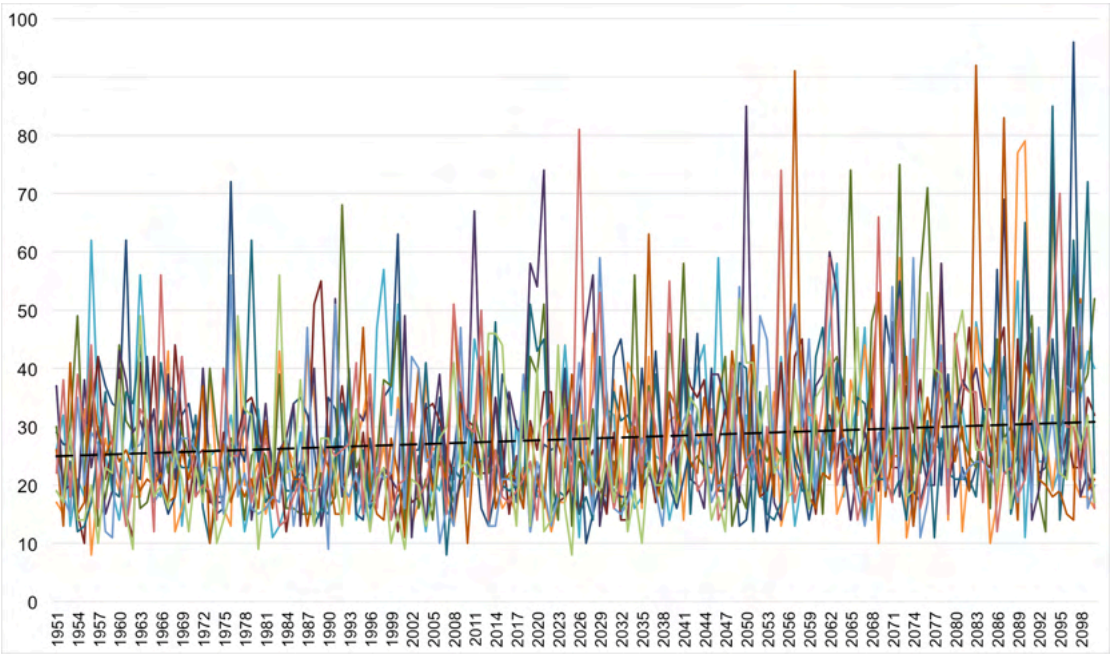

Figure 35: Number of consecutive wet days (> 1 mm) per year in the NSRB above Edmonton.

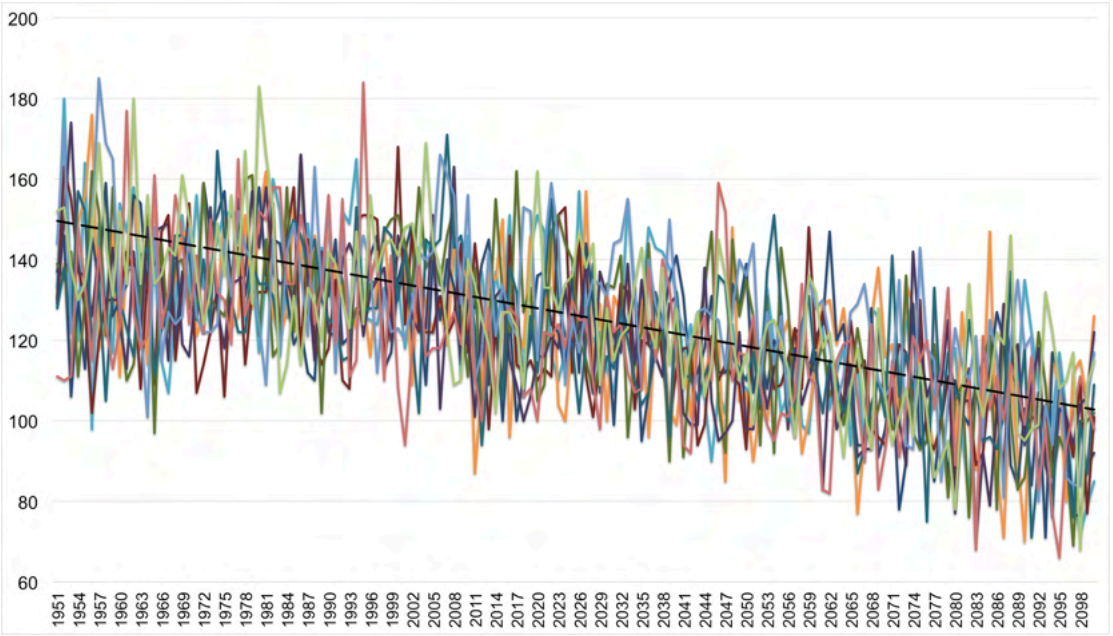

Figure 36: Number of dry days (< 1 mm) per year in the NSRB above Edmonton.

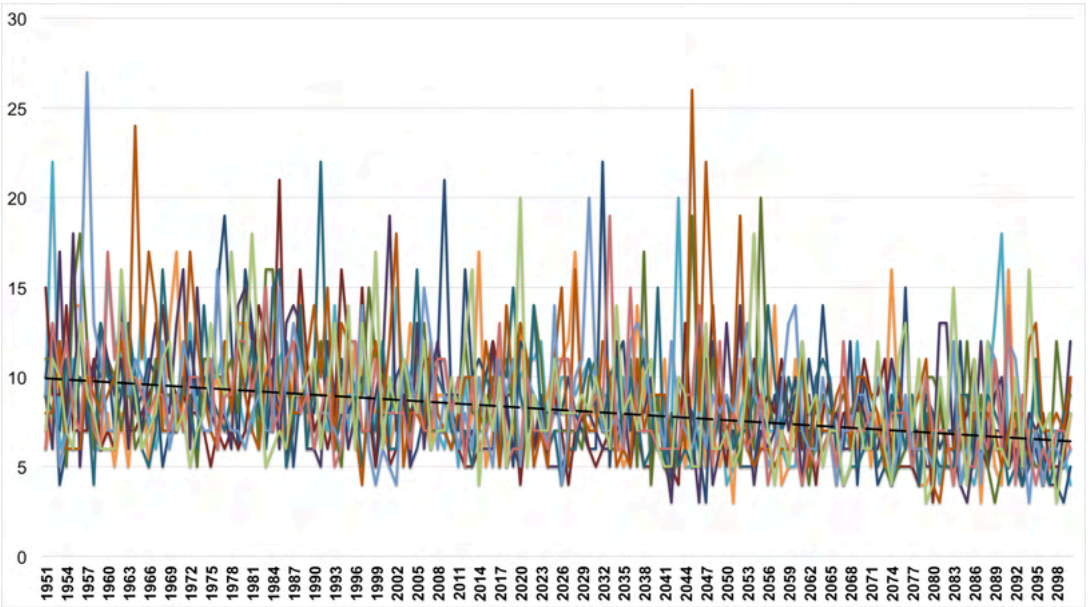

Figure 37: Number of consecutive dry days (< 1 mm) per year in the NSRB above Edmonton.

These shifts in the amount and frequency of precipitation have implications for stormwater runoff and flooding, although projections of these hydrologic extremes also require information on urban hydrology, drainage infrastructure, and river hydraulic and thus are beyond the immediate scope of this project. However, using models of climate and watershed hydrology, we are able to research changes in the timing and amount of runoff in the NSRB above Edmonton, and river levels in the

City. EPCOR Water Canada funded PARC to examine the impacts of a changing climate on the flow of the North Saskatchewan River. This recently completed study of the NSRB above Edmonton (Anis et al., 2021; Sauchyn et al., 2020) and our current research focused on climate change in the EMR are closely related (as acknowledged by EPCOR in a letter of support for the project documented here). Therefore we conclude this section of the report by referring to some of the most relevant results from the other project, placing them in the context of the results of our current project.

Figures 38 to 41 present output from the hydrological modeling of the NSRB above Edmonton using the MESH land surface model and the ensemble of CanRCM4 bias-corrected data as the future climatology. The methods and other results are described in Anis et al. (2021) and Sauchyn et al. (2020). Figure 38 is a time series of the mean annual flow of the NSR from 1951 to 2100. The shading encompasses the ensemble of runoff simulations. The upward trend in the ensemble mean (solid line) is relatively small and thus the more important finding if the expanded range of river levels. This changed river hydrology is consistent with the climate projections of increased winter and spring precipitation and number of wet days presented above. The rising mean river levels are despite the loss of glacier ice and high elevation snowpack in the headwaters of the NSRB, which causes earlier peak river flows, increased winter water levels and lower summer flows. These changes to timing of runoff are discussed in Anis et al. (2021).

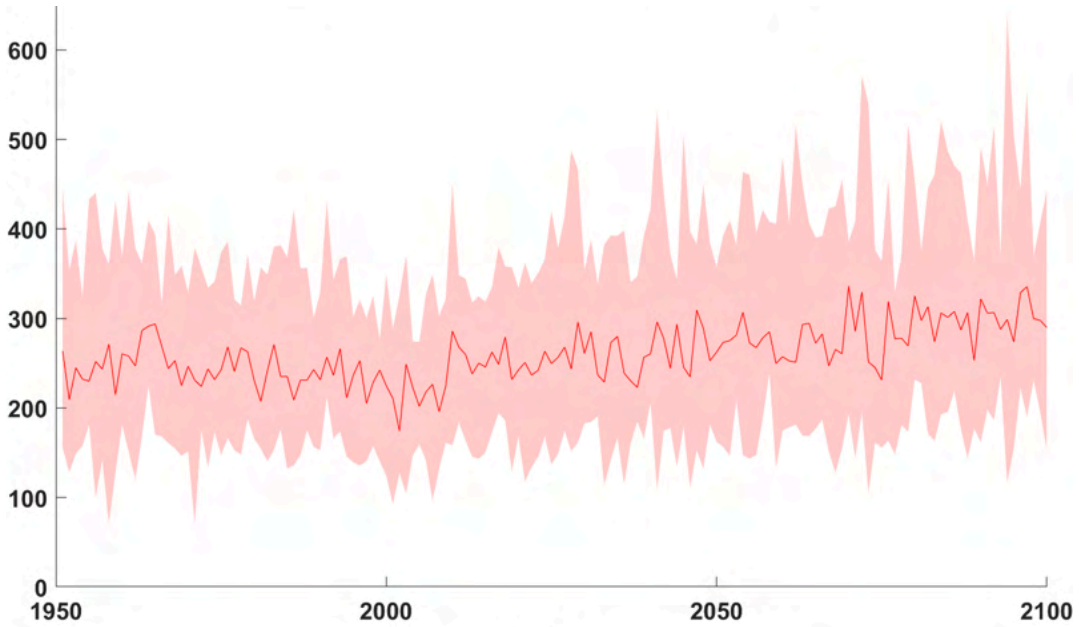

Figure 38: Mean annual flow (m^3/s) of the North Saskatchewan River at Edmonton from the MESH hydrological model and a 15-member ensemble of bias corrected CanRCM4 under RCP8.5 scenario. The solid line is the ensemble mean. Revised from Sauchyn et al. (2020).

Most relevant to adaptation planning in the City of Edmonton is the frequency and timing of extreme river levels. In Figure 39, the ensemble of baseline (1951-2010) and future (2041-2100) frequency distributions of daily low and high river flows indicate a shift in the tails of distribution towards more extreme river flows. Figures 40 and 41 are time series plots of the magnitude and timing of the lowest and highest flows reached each year. There are important shifts in timing as indicated by colour coding of the months. Whereas historically, minimum river flows occurred in winter, in the future they occur in late summer and fall. There is a shift in high flows from summer and early fall to spring, reflecting the loss of glacier and mountain snowpack runoff and increased precipitation in winter and spring.

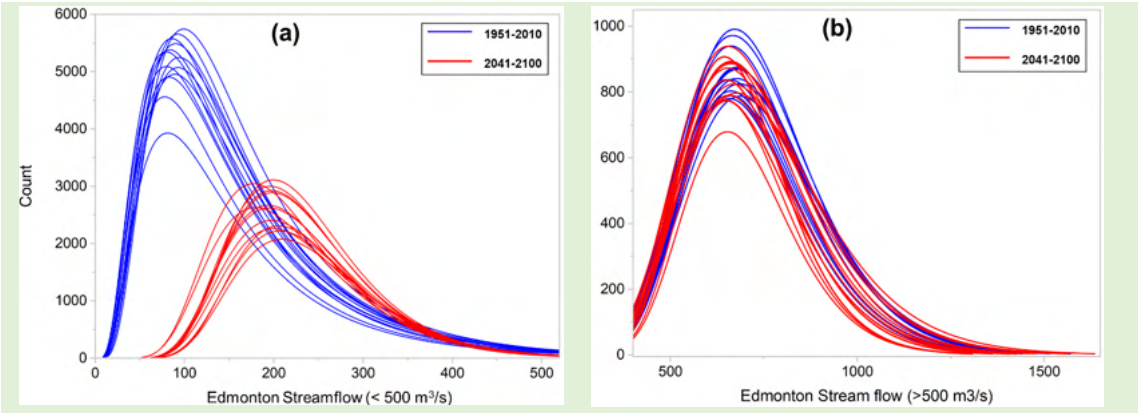

Figure 39: Frequency distributions of daily (a) low and (b) high flows of the NSR at Edmonton for a baseline (1951-2010) and future (2041-2100) periods. From: Sauchyn et al. (2020)

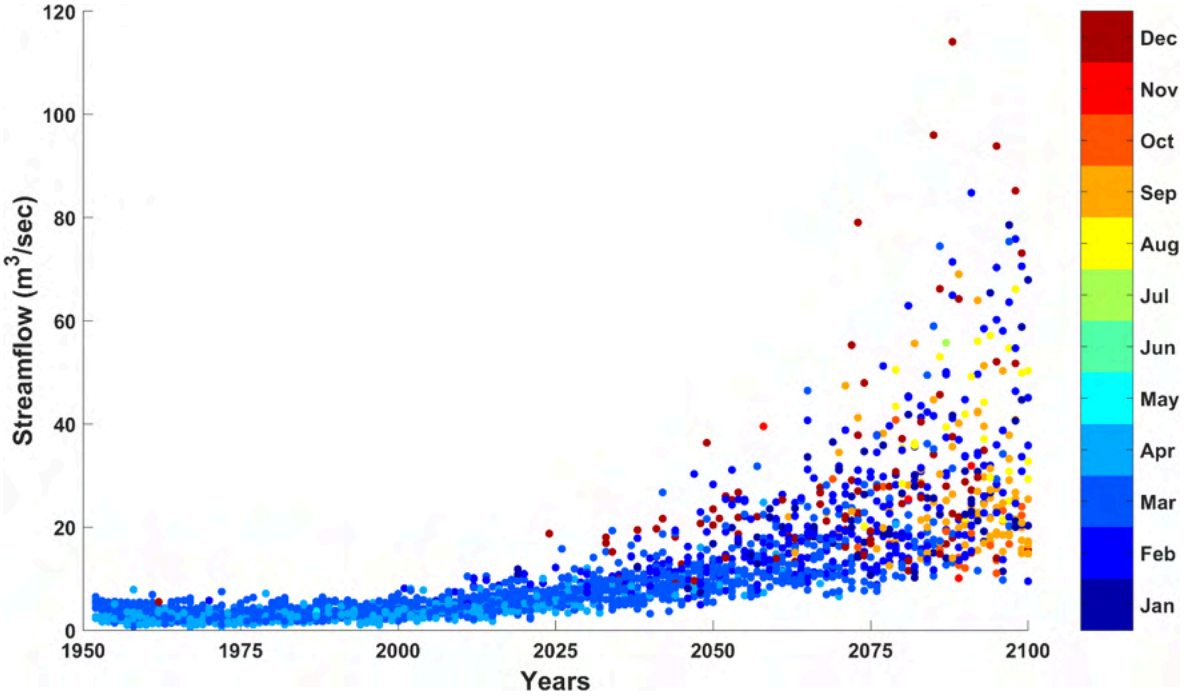

Figure 40: Annual low flows of the NSR at Edmonton from 1950 – 2100. These data are from the MESH hydrological model and a 15-member ensemble of bias-corrected CanRCM4 data (RCP8.5). From: Sauchyn et al. (2020)

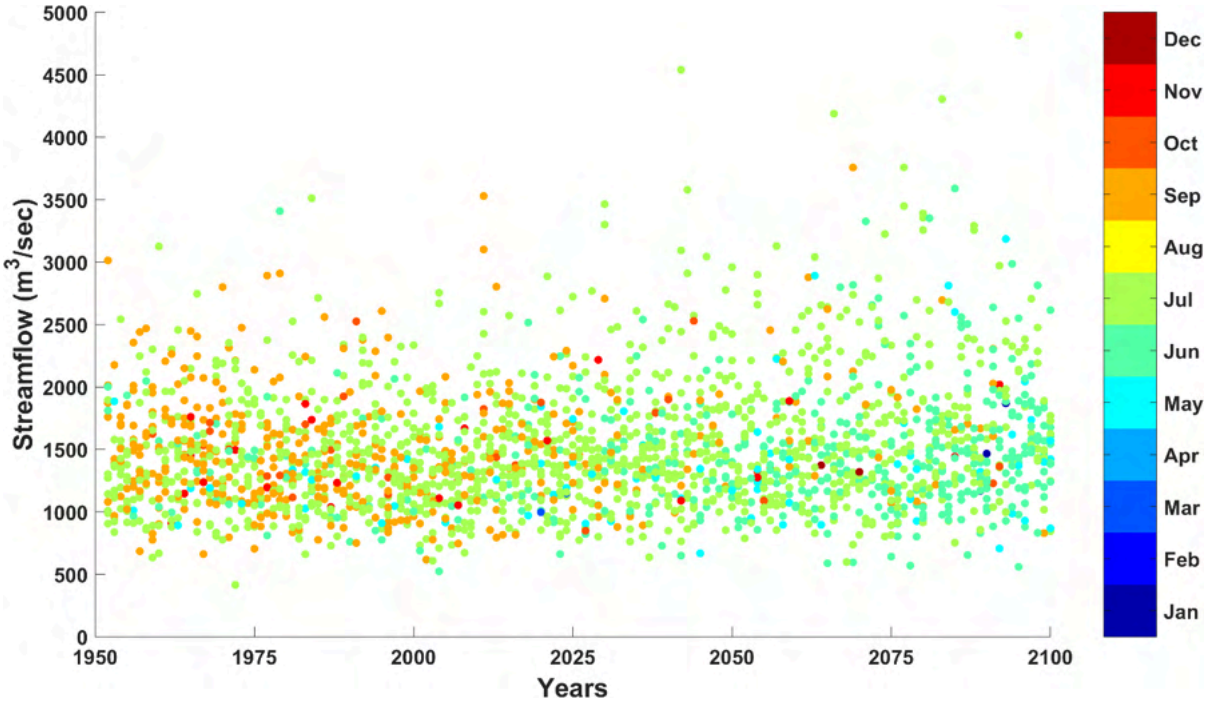

Figure 41: Annual high flows of the NSR at Edmonton from 1950 – 2100. These data are from the MESH hydrological model and a 15-member ensemble of bias-corrected CanRCM4 data (RCP8.5). From: Sauchyn et al. (2020)

5 Discussion: The Implications of our Findings

This project provides the City of Edmonton with a unique database of climate projections at a municipal scale. To achieve this high-resolution (3.3 km), we used the WRF regional climate model to downscale bias-corrected data from the Community Earth System Model (ESM). The result was information of unprecedented detail enabling the mapping of spatial fields across the EMR, and the analysis of climate variables at monthly and daily time steps. This time- and computing-intensive research came with a trade-off. Our CESM-WRF simulation produced a single set of future climates. We offset this limitation in the number of simulations by incorporating data from another 11 ESM/RCM experiments of comparable resolution (25 km) to the 30 km WRF domain. We also used data from a 15-member ensemble of runs of one model - CanRCM4.

This multi-model and ensemble approach was intentional to address the research objectives and scientific questions concerning the interaction of natural climate variability and anthropogenic climate change. We controlled for uncertainty related to the degree of anthropogenic climate change by using a single GHG emission scenario

throughout our modeling and analysis of climate change. RCP8.5 is a high emission scenario. It is a commonly used because global GHG emissions continue to escalate and have yet to level off, and thus RCP8.5 represents a worst-case scenario. By using a single GHG emission scenario, but multiple models, we are able to provide a range of climate projections that reflects different schemes for the numerical modeling of climate. Agreement among different models represents a robust projection. Differences among the 15 CanRCM4 simulations, on the other hand, represent natural variability of the regional climate regime, since use of one model and RCP controls for uncertainty related to the use of different models and emission scenarios.

A large body of recent research (e.g., Deser et al. 2012a, 2012b, 2014; McKinnon and Deser, 2018; Lehner et al., 2020; Thompson et al., 2015) suggests that the contribution of internal climate variability to climate modeling uncertainty has been underestimated. Despite large increases in computing capacity, and corresponding advances in the numerical modeling of global and regional climate, there has not been a commensurate improvement in the precision of the models. This is largely due to "irreducible" internal variability in the climate system:

> *Natural climate variability poses inherent limits to climate predictability … contributes substantial uncertainty to temperature and precipitation trends over North America, especially in winter at mid and high latitudes… [It] is unlikely to be reduced as models improve … (Deser et al. 2012a)*

The mid to high latitudes describes the Canadian Prairies, and winter is the season that produces the precipitation (snow) that accounts for most of the runoff, and the recharge of wetlands, lakes and streams. Barrow and Sauchyn (2019) recently confirmed that natural climatic variability is the dominant source of uncertainty in the prediction of the future climate of western Canada. As shown in Figure 42, it accounts for about 90% of the total variance among climate model projections of future precipitation over the next few decades. The variance explained by differences among models is relatively small and consistent over time. Assumptions about anthropogenic emissions of greenhouse gases (*i.e.,* the GHG emission scenario) become a factor only after mid-century and account for only about 10% of the total variance at the end of the century; natural variability remains dominant.

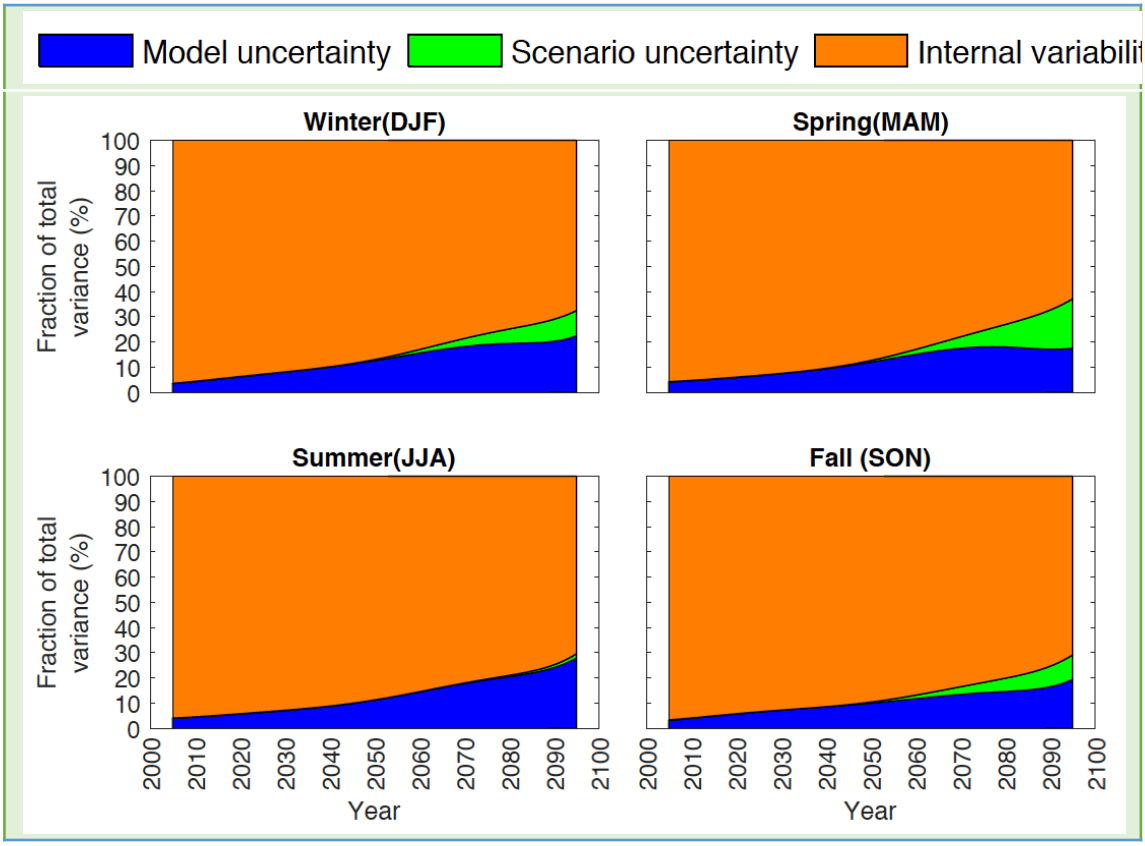

Figure 42: Fraction of the total variance in decadal total seasonal precipitation projections for western Canada. This fraction is attributed to three sources and varies through the 21st century. Source: Barrow and Sauchyn, 2019

These findings of Barrow and Sauchyn (2019) imply that the assessment of climate change and its impacts requires knowledge of both the regional consequences of global warming and the natural variability of the regional climate regime. Inter-annual to decadal variability and extreme hydrologic events present a greater challenge for managing natural resources than incremental slow-onset changes in climate and water. As record climatic variability, instrumental water and weather records span relatively few multi-decadal cycles and coincide with the period of anthropogenic climate change. Paleoclimate records have the advantage of greater record length and pre-dating substantive human interference with the global climate system. Therefore an important component of PARC's climate change research is the tree-ring reconstruction of the paleohydrology of western Canadian River basins. Our current reconstruction of the annual flow of the North Saskatchewan River extends from 888 to 2019. It appears in Figure 43. This paleohydrology captures the full extent of the natural variability of the hydroclimate of the NSRB. The cycling of hydroclimate at inter-annual and decadal scales informs our interpretation of the model projections of the future climate. Thus throughout this report, we emphasized natural variability as a significant source of uncertainty in the projection of regional climate change and we noted where departures from a climate change trend could be attributed to the natural cycling of Alberta's hydroclimate. By explicitly exploring the full range of

uncertainty, and understanding the sources, we can make recommendations for accommodating uncertainty in decision making, including the extent to which existing risk and asset management strategies designed for historical weather events will require adaptation to a shift in hydroclimate variability and frequency / magnitude of extreme events.

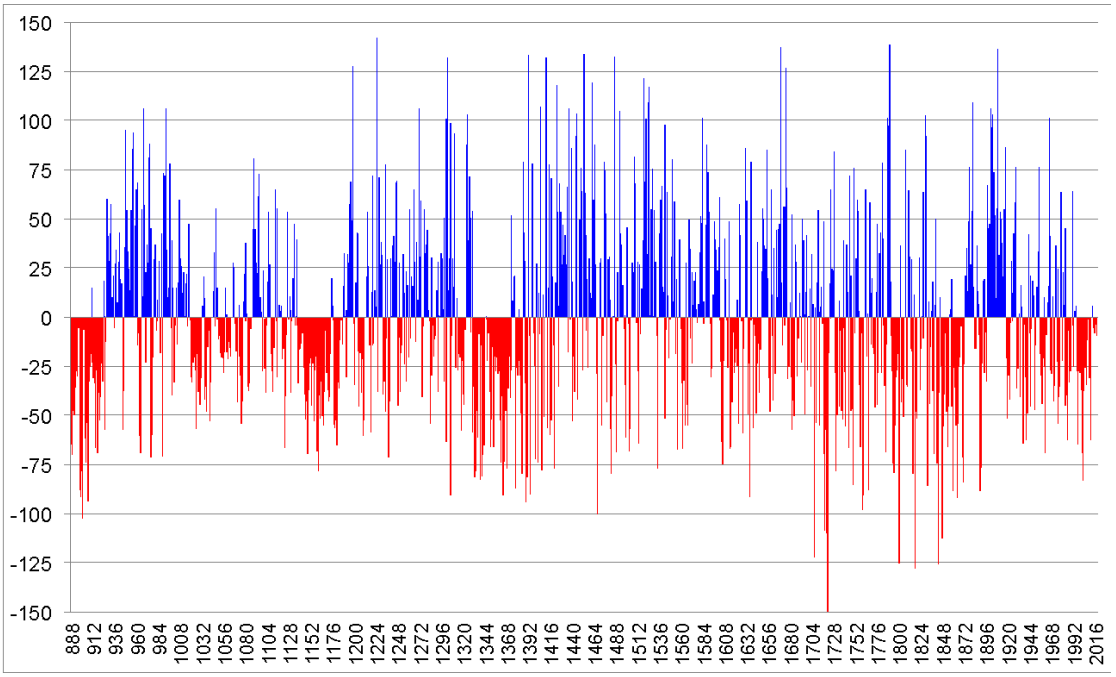

Figure 43: Tree-ring reconstruction of the annual flow of the NSR, 888-2019.

The research team was able to generate large amounts of data about the regional consequences of anthropogenic climate change and underlying natural variability; however, the analysis of these data is context and partner driven. The data are transformed into information and knowledge by applying the requirements of the CoE, and focusing on key hydroclimatic variables and critical thresholds identified in consultation with City staff. The City's Adaptation Strategy and Action Plan (City of Edmonton, 2018) includes "Five Paths to Climate Resilience", each with goals and specific actions. Path 1, "Evidence and Science Based Decisions", is the underlying foundation of Edmonton's approach to climate change adaptation. This path includes an explicit goal of " climate science and evidence based policy and decision making processes" and a stated action to "develop and implement a climate science and evidence based decision-making framework". The Edmonton Declaration, an outcome of the IPCC 2018 Cities and Climate Change Science Conference in March 2018, encourages cities across the globe to take targeted, accelerated and ambitious climate action. It also calls on the science community and other levels of government to provide better data and tools for science-based decision-making.

This project is a response to the call for better data and tools. This technical report is only one of several deliverables. The others will enable the delivery and transfer of

new knowledge arising from this project. These other deliverables are a plain language synthesis document and a workshop which will be the main platform for providing CoE staff with an basic understanding of climate models and methods of constructing climate change projections, including uncertainty and best practices for applying the data.

6 References

Adjusted and Homogenized Canadian Climate Data (AHCCD). 2017. Available online: http://ec.gc.ca/dccha-ahccd/default.asp?lang=En&n=B1F8423

All One Sky (AOS) Foundation. 2018. Edmonton metropolitan region climate resilience exchange: State of knowledge summary. October 30, 2018.

Anis, M. Rehan; Yuliya Andreichuk, Samantha A. Kerr, David J. Sauchyn. 2020. Climate Change Risks to Water Security in Canada's Western Interior, In: Proceedings of the Roorkee Water Conclave 2020, Springer.

Barrow, EB. and Sauchyn, DJ. 2019. Uncertainty in climate projections and time of emergence of climate signals in western Canada. The International Journal of Climatology. doi:10.1002/joc.6079.

Basu, Soumik; David Sauchyn, and Muhammad Rehan Anis. 2020. A Comparative Case Study of the Hydrological Extremes in the Canadian Prairies in the Last Decade due to the ENSO Teleconnection, Accepted for Publication in Water.

Bruyère C. L., J. M. Done, G. J. Holland, and S. Fredrick, 2014: Bias Corrections of Global Models for Regional Climate Simulations of High-Impact Weather. Clim. Dyn., 43, 1847-1856 (DOI: 10.1007/s00382-013-2011-6)

City of Edmonton (2018) Climate Resilient Edmonton: Adaptation Strategy and Action Plan, 48 pp.

CRC Climate Resilience Consulting, (n.d.) Climate Change in the Edmonton Region: Trends And Projections, 69 pp.

Deser C, Knutti R, Solomon S, Phillips AS (2012a) Communication of the role of natural variability in future North American climate. Nat Clim Change 2:775–779, https ://doi.org/10.1038/ nclim ate15 62

Deser C, Phillips A, Bourdette V, Teng H (2012b) Uncertainty in climate change projections: the role of internal variability. Clim Dyn 38:527–546. https ://doi.org/10.1007/s0038 2-010-0977-x

Deser, C., A. S. Phillips, M. A. Alexander, and B. V. Smoliak, 2014: Projecting North American climate over the next 50 years: Uncertainty due to internal variability. J. Climate, 27, 2271–2296, https://doi.org/10.1175/JCLI-D-13-00451.1.

Golder Associates Ltd. 2008. Assessment of climate change effects on water yield from the North Saskatchewan River Basin.

Hong, S.–Y.; Lim, J.-O. J. The WRF single–moment 6–class microphysics scheme (WSM6), Journal of Korean Meteorological Society, 2006, 42, 129–151.

IPCC (2013) Climate Change: The Physical Basis, Contribution of Working Group I to the IPCC Fifth Assessment Report.

Janjic, Z. I. (1996) The surface layer in the NCEP eta model", Proc. 11th Conf. Numer. Weather Prediction, pp. 354-355, Aug.

Janjic, Z. I. (2001) Nonsingular implementation of the Mellor-Yamada level 2.5 scheme in the NCEP meso model, National Centers for Environmental Prediction (U.S.) Office note 437.

Jiang, R., Gan, TY., Xie, J., Wang, N. and Kuo, CC. 2017. Historical and potential changes of precipitation and temperature of Alberta subjected to climate change impact: 1900–2100. Theoretical and Applied Climatology, 127(3-4):725-739.

Kain, J. S., The Kain–Fritsch convective parameterization: An update, J. of App. Met., 2004, 43, 170–181. doi:10.1175/1520-0450(2004)043<0170:TKCPAU>2.0.CO;2

Kienzle, SW., Nemeth, MW., Byrne, JM. and MacDonald, RJ. 2012. Simulating the hydrological impacts of climate change in the upper North Saskatchewan River Basin, Journal of Hydrology, 412–413:76–89.

Lehner, F., Deser, C., Maher, N., Marotzke, J., Fischer, E. M., Brunner, L., Knutti, R., and Hawkins, E.: Partitioning climate projection uncertainty with multiple large ensembles and CMIP5/6, Earth Syst. Dynam., 11, 491–508, https://doi.org/10.5194/esd-11-491-2020, 2020.

MacDonald, RJ., Byrne, JM., Boon, S. and Kienzle, SW. 2012. Modelling the potential impacts of climate change on snowpack in the North Saskatchewan River Watershed. Water Resources Management, 26:3053-3076. doi:10.1007/s11269-012-0016-2.

McKinnon, K. A and C. Deser, 2018: Internal variability and regional climate trends in an observational large ensemble. J. Climate, DOI: 10.1175/JCLI-D-17-0901.1

Mearns, L.O., et al., 2017: *The NA-CORDEX dataset*, version 1.0. NCAR Climate Data Gateway, Boulder CO, accessed 02 December 2019, https://doi.org/10.5065/D6SJ1JCH

Monaghan, A. J., D. F. Steinhoff, C. L. Bruyere, and D. Yates. 2014. NCAR CESM Global Bias-Corrected CMIP5 Output to Support WRF/MPAS Research. Research Data Archive at the National Center for Atmospheric Research, Computational and Information Systems Laboratory. https://doi.org/10.5065/D6DJ5CN4. Accessed† 10/09/2019.

Nakanishi, M.; Niino, H. Development of an improved turbulence closure model for the atmospheric boundary layer, J. of Met. Soc. of Jap., 2009, 87, 895–912. doi:10.2151/jmsj.87.895

Olson, J.B.; Kenyon, J. S.; Angevine, W. M.; Brown, J. M.; Pagowski, M.; Sušelj, K. A Description of the MYNN-EDMF Scheme and the Coupling to Other Components in WRF–ARW. NOAA Technical Memorandum OAR GSD, 2019, 61, pp. 37. doi:10.25923/n9wm-be49

Sauchyn, D., Davidson, D., and Johnston, M. 2020. (In Press). The Prairie Provinces. In Natural Resources Canada. Canada in a Changing Climate: Advancing our Knowledge for Action. Ottawa: Natural Resources Canada.

Sauchyn, David; Muhammad Rehan Anis, Soumik Basu, Yuliya Andreichuk, Sunil Gurrapu, Samantha Kerr, and Juan Mauricio Bedoya Soto (2020) Natural and Externally Forced Hydroclimatic Variability in the North Saskatchewan River Basin: Support for EPCOR's Climate Change Strategy Final Report to EPCOR Water Canada, September, 2020, 99 pp.

Sauchyn, DJ; J Vanstone, J-M St. Jacques, R Sauchyn. 2015. Dendrohydrology in Western Canada and Applications to Water Resource Management. Journal of Hydrology, 529: 548-558.

Skamarock, WC; JB Klemp, J Dudhia, DO Gill, Z Liu, J Berner, W Wang, JG Powers, MG Duda, DM Barker, and X-Y. Huang, 2019: A Description of the Advanced Research WRF Version 4. NCAR Tech. Note NCAR/TN-556+STR, 145 pp. doi:10.5065/1dfh-6p97.

Tewari, M.; Chen, F.; Wang, W.; Dudhia, J.; LeMone, M. A.; Mitchell, K.; Ek, M.; Gayno, G.; Wegiel, J.; Cuenca, R. H. Implementation and verification of the unified NOAH land surface model in the WRF model. 20th conference on weather analysis and forecasting/16th conference on numerical weather prediction, 2004, 11–15.

Thompson, D. W. J., Barnes, E. A., Deser, C., Foust, W. E., and Phillips, A. S. (2015). Quantifying the Role of Internal Climate Variability in Future Climate Trends. J. Clim. 28, 6443–6456. doi:10.1175/JCLI-D-14-00830.1.

Vincent, LA., Wang, XL., Milewska, EJ., Wan, H., Yang, F. and Swail, V. 2012. A second generation of homogenized Canadian monthly surface air temperature for climate trend analysis. Journal of Geophysical Research, 117:D18110. doi:10.1029/2012JD017859.

Xu, K. and Randall, D.A. 1996. A Semiempirical Cloudiness Parameterization for Use in Climate Models. J. Atmos. Sci., 53, 3084–3102, https://doi.org/10.1175/1520-0469(1996)053<3084:ASCPFU>2.0.CO;2